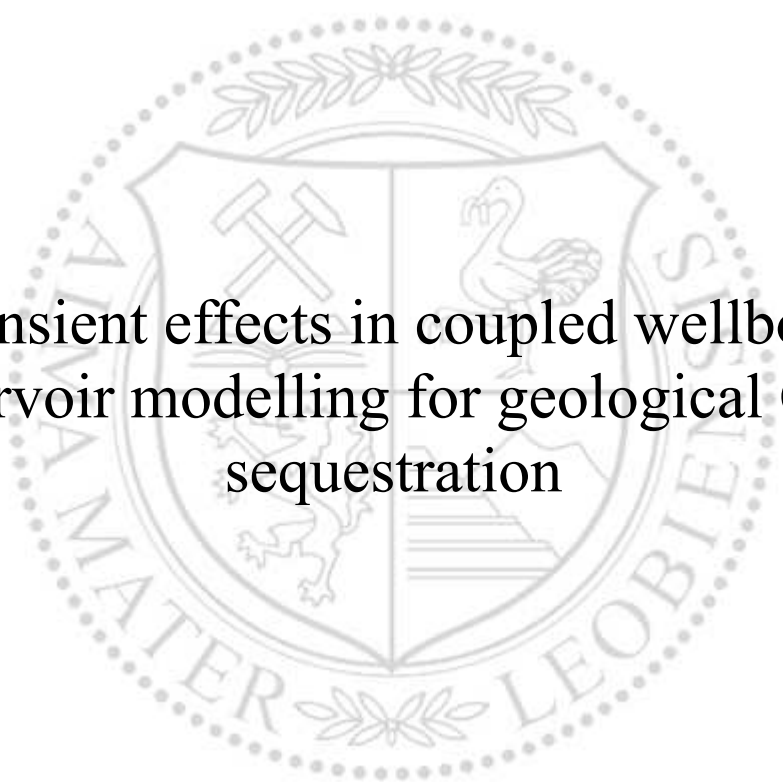Chair of Reservoir Engineering

Master's Thesis

Transient effects in coupled wellbore-reservoir modelling for geological CO2 sequestration

Jose Kevin Pauyac Estrada

August 2023

AFFIDAVIT

I declare on oath that I wrote this thesis independently, did not use other than the specified sources and aids, and did not otherwise use any unauthorized aids.

I declare that I have read, understood, and complied with the guidelines of the senate of the Montanuniversität Leoben for "Good Scientific Practice".

Furthermore, I declare that the electronic and printed version of the submitted thesis are identical, both, formally and with regard to content.

Date 30.08.2023

_____
Signature Author
Jose Kevin Pauyac Estrada

Jose Kevin Pauyac Estrada
Master's Thesis 2023
Petroleum Engineering

Transient effects in coupled wellbore-reservoir modelling for geological CO2 sequestration

Supervisor: Dr. Siroos Azizmohammadi
Co-supervisor: Dr. Holger Ott
Advisor: Dr. Oleksandr Burachok

Chair of Reservoir Engineering

dpe   MONTAN
UNIVERSITÄT
LEOBEN

I dedicate my dissertation work to my respectful and beloved parents and sister without whose constant support and guidance and unconditional love this work was not possible. They were always my inspiration. I am really thankful for having you in my life.

I also want to dedicate this dissertation work to my company's mentor Oleksandr Burachok under whose constant guidance, trust, and patience I could write this work. He not only enlightened me with academic knowledge for my future career but also gave me valuable values. I am thankful for having given me the opportunity to work with you

Acknowledgments

Abstract

The energy sector actively seeks eco-friendly solutions to mitigate the environmental repercussions of oil and gas operations. One of these solutions is Carbon, Capture, and Storage technology (CCS). However, this technology is still under development by experts in the field. There have been several research studies on this behalf to study and comprehend the CO2 fluid flow behavior when traveling from the surface to the porous media.

CCS is a promising technology for mitigating greenhouse gas emissions and addressing the challenges of climate change. The process involves capturing CO2, transporting it to the designated storage sites, and subsequently injecting it into subsurface formations for safe long-term geological sequestration.

As CO2 flows along the wellbore from the surface to the storage formation, the CO2 undergoes different thermal processes. For example, CO2 can undergo phase transition; hydrates can form depending on the injection conditions of pressure and temperature at the surface; a cooling effect can happen when reaching the storage formation (Joule-Thomson effect); salt can precipitate in the near-wellbore area, reducing the porosity, and thus, compromising the CO2 injectivity.

Effective and practical implementation of CCS in the real world requires a deep understanding of the wellbore dynamics coupled to the reservoir domain. However, most standard petroleum software focuses on multiphase fluid flow behavior under steady-state conditions, considering only the wellbore or the reservoir domain. Therefore, there is a growing imperative to develop models where transient phenomena are studied in a jointly wellbore-reservoir domain.

This work investigates the transient effects associated with CO2 injection, particularly emphasizing contrasting gas and supercritical CO2 injection. The distinct behaviors impact the CO2 injectivity, especially concerning salt precipitation or hydrate formation. To achieve this, the research employs the numerical software T2Well – an advanced transient simulator designed to analyze coupled wellbore-reservoir dynamics.

Results showed that no matter in which state the CO2 is injected, it will reach the reservoir in the supercritical phase due to the phase transition occurring in the wellbore at early simulation time. Moreover, injecting supercritical CO2 is preferred over gas CO2. In the gas CO2 case,

higher salt precipitation can be noticed, and a stronger JT-effect cooling effect is appreciated in the near-wellbore area than in the supercritical CO2 case.

This Master's thesis contributes to an enhanced comprehension of transient processes and empowers informed decision-making for the practical application for real-world CCS technology implementation.

Zusammenfassung

Der Energiesektor sucht aktiv nach umweltfreundlichen Lösungen, um die Umweltauswirkungen der Öl- und Glasindustrie zu mildern. Eine dieser Lösungen ist die Carbon-, Capture- und Storage-Technologie (CCS) welche sich allerdings noch in der Entwicklungsphase befindet. In diesem Zusammenhang wurde eine Forschungsstudie durchgeführt, um das Strömungsverhalten von Kohlenstoffdioxid (CO_2) auf dem Weg von der Oberfläche zum porösen Gestein zu untersuchen und zu verstehen.

CCS ist eine vielversprechende Technologie zur Minderung von Treibhausgasemissionen und zur Bewältigung der Herausforderungen des Klimawandels. Der Prozess umfasst die Extraktion von CO_2 aus industriellen Emissionen oder der Atmosphäre, den Transport zu den vorgesehenen Speicherorten und die anschließende Injektion in unterirdische Formationen zur langfristigen geologischen Speicherung.

Während CO_2 entlang des Bohrlochs von der Oberfläche zur Speicherformation fließt, durchläuft das CO_2 verschiedene thermische Prozesse. Beispielsweise kann CO_2 einen Phasenübergang durchlaufen; abhängig von den Injektionsbedingungen, dem Druck und der Temperatur an der Oberfläche, können sich Hydrate bilden; beim Erreichen der Speicherformation kann ein Kühleffekt auftreten (Joule-Thomson-Effekt) und zudem kann es zu bohrlochnahen Salzablagerungen kommen, welche die Porosität verringern und somit die CO_2-Injektivität signifikant beeinträchtigen.

Eine effektive und praktische Umsetzung von CCS in der realen Welt erfordert ein tiefes Verständnis der Strömungsmechanik und Thermodynamik im Bohrloch, welche stark von dem Verhalten der Lagerstätte beeinflusst werden. Der Großteil der konventionellen Programme zur Simulation von Erdöl und Erdgas Lagerstätten konzentriert sich jedoch auf das mehrphasige Strömungsverhalten unter stationären Bedingungen und berücksichtigt daher nur den Bohrloch- oder Lagerstättenbereich. Daher besteht ein wachsender Bedarf an der Entwicklung von Modellen, welche in der Lage sind, instationäre Phänomene in einem gekoppelten Bohrloch-Reservoir Kontext zu untersuchen.

Diese Arbeit untersucht daher die transienten Effekte im Zusammenhang mit der CO_2-Injektion, wobei der Schwerpunkt insbesondere auf dem Vergleich der Injektion von Gas und überkritischem CO_2 liegt. Die unterschiedlichen Verhaltensweisen wirken sich auf die CO_2

Injektivität aus, vor allem hinsichtlich der Salzausfällung oder Hydratbildung. Dafür wird im Rahmen dieser Studie mit dem numerischen Simulationsprogramm T2Well gearbeitet – bei welchem es sich um eine führende Software zur Analyse gekoppelter Bohrloch-Reservoir-Dynamik handelt.

Die Ergebnisse zeigen, dass das CO2 unabhängig vom initialen Aggregatszustand, in dem es injiziert wird, aufgrund des Phasenübergangs, der im Bohrloch zu einem frühen Simulationszeitpunkt stattfindet, in der überkritischen Phase das Reservoir erreicht. Darüber hinaus wird die Injektion von überkritischem CO2 gegenüber gasförmigem CO2 bevorzugt. Im Fall von gasförmigem CO2 konnte eine höhere Salzausfällung festgestellt werden, zudem ist im bohrlochnahen Bereich ein stärkerer Joule-Thomson-Kühleffekt zu erwarten als bei überkritischem CO2.

Diese Masterarbeit trägt zu einem verbesserten Verständnis instationärer Strömungsphänomene bei und ermöglicht daher eine fundierte Entscheidungsfindung für die praktische Implementierung der CCS-Technologie.

Table of Contents

Chapter 1

Introduction

1.1   Background and Context

Due to human activity and the development of the industrial sector, the amount of greenhouse gases in the atmosphere that causes this phenomenon has become alarmingly large over a very short time. The increase in the proportion of greenhouse gases above normal concentrations mainly causes an increase in temperature on Earth, being very detrimental to life. For this reason, the need has arisen to reduce the emissions of these greenhouse gases, such as methane, CO_2, among others, and thus be able to avoid the disappearance of all life on Earth.

Before the Industrial Revolution, greenhouse emissions were very low. These emissions grew relatively slowly until the mid-20th century when 6 billion tonnes of CO_2 were emitted. However, emissions were quadrupled by the end of the 20th century, reaching almost 25 billion tonnes (Ritchie et al., 2020). Figure 1.1 shows the annual CO_2 emissions worldwide from 1750 to 2021.

Several research studies were carried out to find new technologies to counteract greenhouse emissions. Carbon Capture and Storage (CCS) is a promising technology to mitigate global warming. Several processes are carried out during CCS. First, the CO_2 should be captured, usually from industrial sources. Then, the captured CO_2 is transported to the field for its injection and long-term sequestration in deep subsurface formations (Global CCS Institute, 2015).
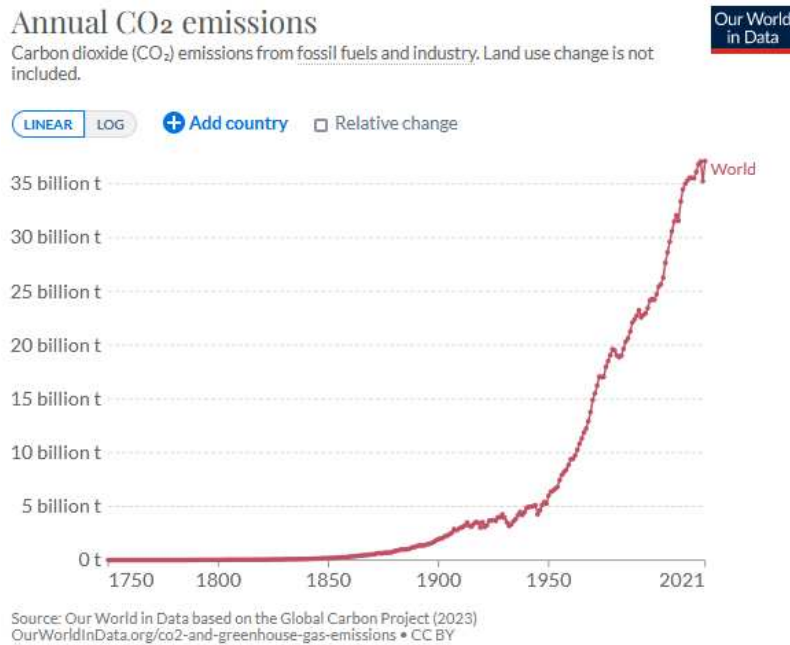
Figure 1.1.1 World's annual CO2 emissions from 1750 to 2021 (Ritchie et al., 2020)

Preferable subsurface formations for CO2 injection are depleted gas reservoirs or saline aquifers. In order to store the CO2 safely in the subsurface and prevent it from going back into the atmosphere, studies and simulations must be carried out. It is crucial to understand the behavior and performance of CO2 when flowing from the surface to the formation.

Traditionally, software were developed considering only the wellbore or the reservoir domain. Generally, numerical multiphase fluid flow simulation is considered from the reservoir to the surface through the wellbore. Usually, most wellbore simulators like Prosper from Petroleum Experts Limited (Petroleum Experts, 2013) assume a constant flow rate for the inflow of reservoir fluid to the well and use steady-state values for the BHP as a function of the fluid flow rates and WHP.

In a non-coupled simulation, the time response of the reservoir and wellbore are not the same. The time response from the reservoir processes is usually on a time scale from hours to decades (such as, while the time response from the wellbore processes (such as multiphase fluid flow, temperature, and pressure propagation) takes seconds or tens of minutes (Da Silva and Jansen, 2015).

Nevertheless, the simulation may face some problems due to an overlap in response time scales, especially near the well region in the reservoir. Therefore, coupled wellbore-reservoir numerical simulators are needed, like T2Well or CoFlow from CMG Group.

For instance, in coupled wellbore-reservoir simulations, the reservoir model is considered a plug-in to the wellbore model (Hu and Chupin, 2007). During the simulation, the boundary

conditions are provided by the wellbore model (which controls the integrated simulation), while the flow rate, which can be either negative or positive in case the model is either injection or production, is calculated by the reservoir model.

Understanding the CO_2 flow dynamics in a system under a non-equilibrium (transient) state is also essential for accurate prediction of CO_2 injection and storage behavior. Transient simulations are crucial for the prediction of the well's behavior. Several research studies have been carried out to model CO_2 injection using a transient wellbore-reservoir simulator. Satim et al. studied the flow behavior caused by transient procedures using the coupled wellbore-reservoir simulator GPAS (General Purpose Adaptive Simulator) (Santim et al., 2020). Wan et al. developed a transient model to study the phase state in CO_2 injection wells using the finite difference method (Wan et al., 2021).

Therefore, this thesis aims to analyze the transient effects and the near wellbore-area effects in coupled wellbore-reservoir modeling for long-term geological CO_2 sequestration. A conceptual model will be studied to compare the advantages and disadvantages of injecting CO_2 in the gas and supercritical phase using T2Well/ECO2N.

1.2   Scope and Objectives

The objective of this thesis is to investigate the transient and near wellbore-area effects in coupled wellbore-reservoir modeling for CO_2 geological sequestration. To achieve this goal, existing literature on wellbore-reservoir modeling has been reviewed. Also, a conceptual model will be built to study the fluid flow behavior when injecting gas and supercritical CO_2 into an aquifer using the transient wellbore-domain coupled to the reservoir-domain simulator T2Well with the equation of state (EOS) module ECO2N.

Chapter 2

Literature Review

For many years global economies have been dependent on fossil fuels, i.e., oil, gas, coil, as the main energy source (Magalhães Pires, 2019). Even though exploitation of these sources may meet each country's energy demand to a large extent, it emits giant amount of greenhouse gases, leading to an increase of temperature worldwide.

Over the last 100 years, the global mean surface temperature has increased by 0.74 ± 0.18 °C. Moreover, the rate of warming over the last 50 years (0.13 ± 0.02 °C per decade) is double that over the last 100 years (0.07 ± 0.02 °C per decade) (Singh, 2013).

To avoid further impacts, countries around the world have joined forces to mitigate this problem. Several studies have been carried out to reduce the CO2 concentration in the atmosphere or even to achieve net-zero emissions, which is the goal of the Paris Agreement (NewClimate Institute & Climate Analytics, 2020).

Three solutions to this environmental problem were proposed (Magalhães Pires, 2019):
• Carbon Capture and Storage
• Energy efficiency improvement
• Renewable Energy

The CCS technology was introduced in 1977 and consists of CO2 capture and injection for its long term into geological formations. According to the International Energy Agency, 17% of global CO2 emission can be reduced by 2050 thanks to this promising technology (Raza et al., 2018).

## 2.1   Carbon Capture and Storage

2.1.1 Definition

Carbon Capture and Storage is an innovative technology focused on reducing CO_2 emissions. The aim is not to let carbon enter the Earth's atmosphere; that way, the further impact of excess greenhouse gases can be prevented.

Once the CO_2 is captured and transported to the storage site, it may be stored in geological formations or oceans. However, even though CO_2 storage in oceans was initially conceived, due to the high negative environmental impact, oceans are no longer an option (Singh, 2013).

Therefore, the potential storage sites for CO_2 are geological structures: saline aquifers and depleted hydrocarbon reservoirs. The preferences for where to store the captured CO_2 depend on several factors, including availability, logistical, and economic concerns (Alkan et al., 2021).

Thus, the CCS technology can be divided into three parts:

a) **CO_2 capture** – various technologies can be used to capture carbon from gases that are produced during different industrial processes. There are three main types of CO_2 capture (Global CCS Institute, 2015):
   1. Pre-combustion – fuel is converted into a gas mixture of hydrogen and CO_2, from which CO_2 is separated and captured.
   2. Post-combustion – CO_2 is separated from the flue gases produced in the air by the combustion of primary fuels after hydrocarbon combustion. A small fraction of the CO_2 in the flue gas stream is typically captured using a liquid solvent.
   3. Oxy-fuel combustion – primary fuels are burned in a pure oxygen atmosphere to produce flue gas, mainly CO_2 and water vapor. CO_2 is then captured once the water vapor is removed from the gas stream by cooling and compressing it.

b) **CO_2 transport** – after carbon capture, it is transported by either ship or pipeline to the storage site for long-term safe storage. Transportation should be safe to avoid release into the atmosphere.

c) **CO_2 storage** – the last step of CCS technology is to store the captured and transported CO_2 in underground sites located several kilometers under the surface.
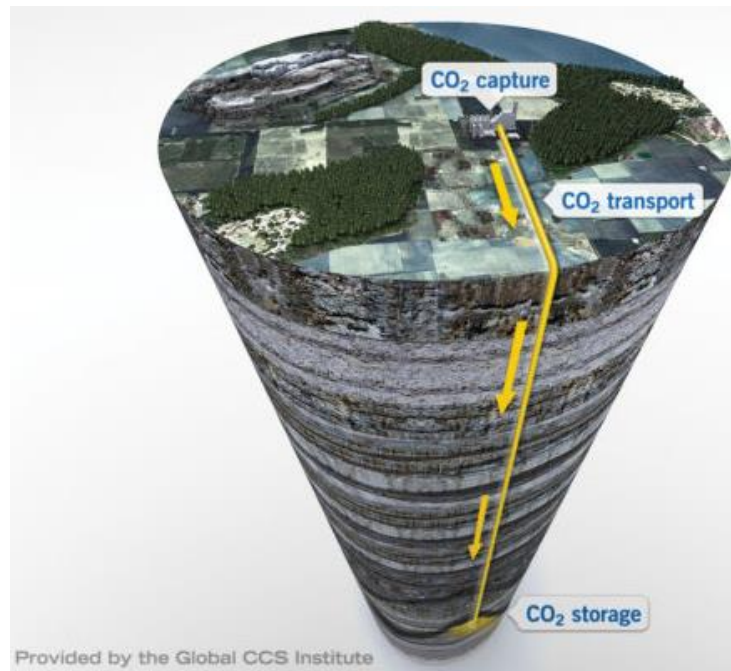
Figure 2.1.1 CCS process (Global CCS Institute)

2.1.2 Trapping mechanisms

After CO2 is captured and transported to the field, it is injected into the subsurface to be trapped and stored safely and permanently.

It is preferable to inject CO2 under supercritical conditions since the density of supercritical CO2 is compared to CO2 in a liquid phase, while viscosity is treated as a gas. The main advantage of storing supercritical CO2 is that the required storage volume is significantly less than storing it at standard conditions. (National Energy Technology Laboratory)

Nevertheless, when flowing from the surface to the reservoir, the CO2 can undergo a phase change. As a result, the CO2 can be stored as compressed gas, liquid, or supercritical, depending on the reservoir conditions.

A suitable CO2 storage reservoir needs a layer of porous rock at the correct depth to hold CO2 sufficient capacity and an impermeable caprock layer to seal the porous layer underneath. Trapping refers to how the CO2 remains underground. There are four main trapping mechanisms: structural, residual, solubility, and mineral (National Energy Technology Laboratory).

   a) **Structural Trapping** – It refers to the physical trapping of CO2 in which the rock layers and faults within and above the storage formation act as seals, preventing CO2 from moving out of the storage formation.
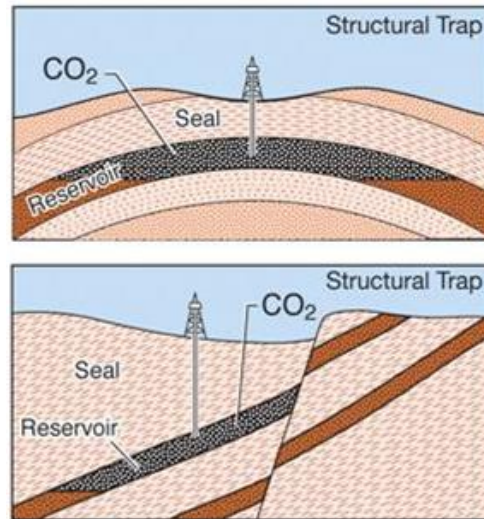
Figure 2.1.2 Structural Trapping (National Energy Technology Laboratory)

Figure 2.1.2 shows two examples of structural trapping. In the top figure, the CO2 is trapped beneath a dome, not being able to migrate laterally or vertically. In the bottom figure, the CO2 is not able to migrate laterally or vertically by the overlying seal rock and a fault to the right of the CO2.

b) **Residual trapping** – Once the supercritical CO2 is injected into the formation, it displaces the existing fluids as it moves through the porous media. As the porous rock acts like a rigid sponge, some droplets will be trapped in the smaller pore spaces becoming immobile, just like water in a sponge.
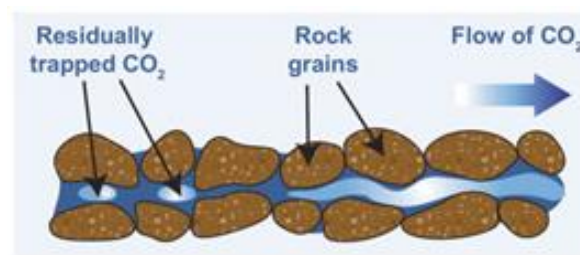

Figure 2.1.3 Residual Trapping (National Energy Technology Laboratory)

c) **Solubility or dissolution trapping** – At this stage, some of the CO2 dissolves into the salty water already in the porous rock. This saltwater containing CO2 is denser than the surrounding fluids so that it will sink to the bottom of the rock formation over time.
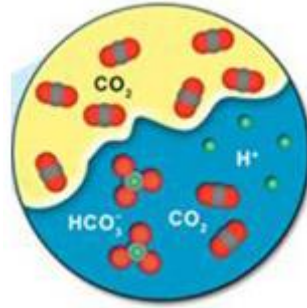
Figure 2.1.4 Solubility Trapping (National Energy Technology Laboratory)

d) **Mineral trapping** – This is the final stage of trapping. The CO2-rich-water forms a weak carbonic acid H2CO3, which over time can react with the minerals in the surrounding rock to form solid carbonate minerals, permanently trapping and storing CO2.
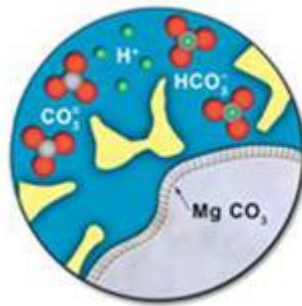

Figure 2.1.5 Mineral Trapping (National Energy Technology Laboratory)

To ensure that a CO2 storage site functions, a rigorous monitoring process begins at the reservoir selection stage and continues for as long as required. In addition, the well caprock and adjacent rock formations are monitored for changes in pressure and CO2 concentration levels. All these systems ensure that response times are swift and decisive and can be taken when necessary. Furthermore, monitoring continues even after a well is abandoned, and EU law requires that stored CO2 is kept safely and permanently underground.

When it comes to reservoir simulation, it is fundamental to understand the fluid behavior, the processes that can happen in both wellbore and reservoir, as well as the changes these domains may be subjected to. T2WELL is a numerical simulator developed to satisfy the need for coupling flow solutions (Vasini et al., 2015).

2.2   CO2 thermodynamic conditions before injection

As seen from Figure 2.1.1, when CO2 is captured, it must be transported to the storage sites. Many of the CO2 capture sites (power stations and industrial plants) are located far from the storage sites. In Europe, for example, the power stations and industrial plants are in inland

continental Europe, while the storage sites are in the North Sea (Roussanaly et al., 2021). Thus, the pressure and temperature conditions of CO_2 at which it reaches the storage sites are important to know the optimum injection conditions from the economical point of view.

Two means of CO_2 transportation can be sorted: pipeline-based transport and tank-based transport. For the first one, CO_2 is usually transported in its supercritical state, while for the tank-based transport, the CO_2 is usually transported in the liquid state in ships, trains, or trucks.

From the economical point of view, CO_2 should be liquefied when transported by ship since it takes from 1 to 5 hundredth of the gaseous CO_2 volume (Seo et al., 2016). Moreover, pipeline-based transport is preferred due to its low cost of transport for large capacities and low-to-medium distances. However, for the past decade, the interest for tank-based CO_2 transport has increased, in particular, the use of ships, since they are cost-effective for small volumes or over long distances due to their lower investment costs, flexibility, and shorter construction time in comparison to pipelines (Roussanaly et al., 2021).

When transporting CO_2 by ship, there is an assumption that CO_2 is transported at "low" pressure (around 7 barg and 46 °C). However, transport at around 15 barg and 30 °C is being implemented based on experience. Pressures above 20 barg are not cost-competitive according to Seo et al.

Roussanaly et al. considered nine scenarios for CO_2 transportation, among them their base case is when CO_2 is liquefied directly after capture – 1 bara and 40 °C after capture, while from inland emitters, the CO_2 would be transported at high pressure via pipeline prior to liquefaction and ship transport – 90 bara and 40 °C after capture.

They carried out a study in which a comparison of transporting CO_2 at a pressure of 7 and 15 barg for a wide range of annual volumes (0.5-20 $MtCO_2$/year) and transport distances (50-200 km) was made. They came to the conclusion that shipping CO_2 at 7 barg is more cost-efficient than at 15 barg (Roussanaly et al., 2021).

In addition, Seo et al. carried out a study to determine the optimal pressure. For this, they proposed seven liquefaction pressures between the CO_2 triple and critical point with increments of 10 bar. They stated that the liquefaction and pumping system costs decreased when increasing the liquefaction pressure, coming to the conclusion that 15 bar and 27 °C are the optimal pressure and temperature conditions with a disposal cost of about 25 USD/ton of CO_2.

2.3   Flow regimes in a multiphase fluid flow

Flow regimes can be classified as transient, pseudo-steady, and steady-state depending on the boundary conditions. These regimes can be identified according to the change in time of any parameter affecting the system, usually pressure. If the pressure change in time is equal to zero, the system is in an equilibrium state or steady-state. Thus, the steady flow regime's mass flow rate is also constant. This regime can be formulated using the following mathematical expression:

$$\frac{\partial p}{\partial t} = 0 \qquad (2.2.1)$$

where $\partial p/\partial t$ represents the change of pressure with time.

Nevertheless, if both reservoir and wellbore pressure does not remain constant with time, changing at a constant rate, the pseudo-steady state flow regime can be identified. In this regime, since the fluid does not flow across the boundaries (Fanchi, 2010), it can be said that the system behaves similarly to a closed system. The pseudo-steady state flow regime can be formulated as:

$$\frac{\partial p}{\partial t} = constant \qquad (2.2.2)$$

The third flow regime is called transient. Distinctively to the other two flow regimes, the transient flow regimes can be identified when pressure changes as a function of time. In this case, no restrictions on fluid movement exist. The mathematical expression which describes this flow regime is the following:

$$\frac{\partial p}{\partial t} = f(t) \qquad (2.2.3)$$

2.4   Near-wellbore effects

When CO_2 is injected into the formation, the system close to the well experiences alterations (near-wellbore effects), impacting the reservoir's geochemical, geomechanical, and thermal state. Thus, these effects impact the flow characteristics, CO_2 containment, and temperature profile (Creusen, 2018). Figure 2.3.1 shows an overview of the main near-wellbore effects.
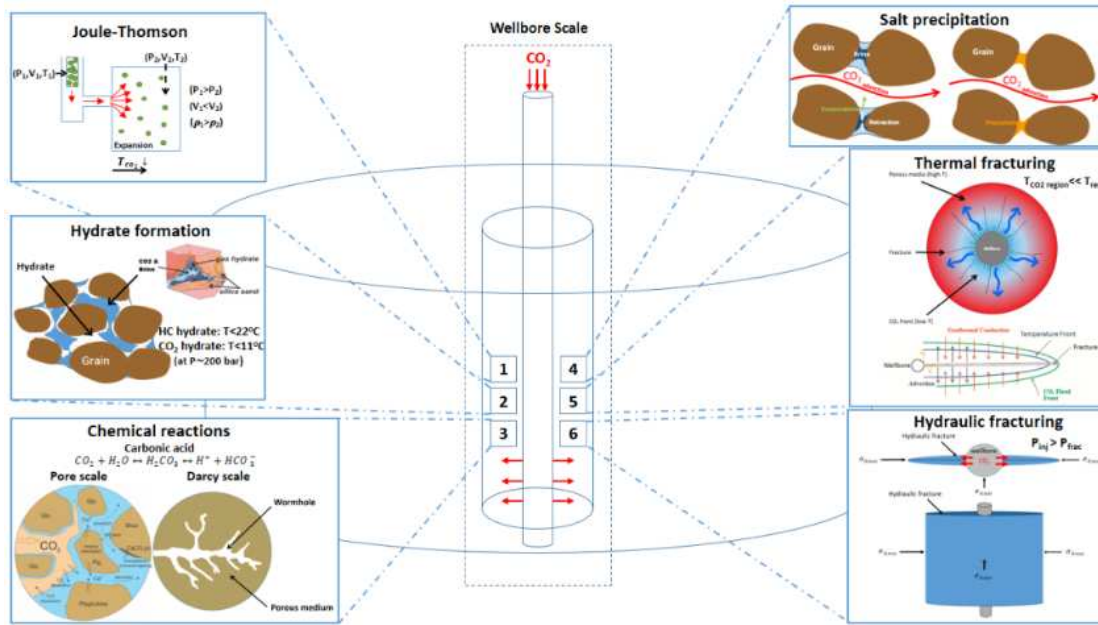
Figure 2.4.1 Near-wellbore effects overview (Creusen, 2018)

2.4.1 Joule-Thomson effect

As stated, depleted hydrocarbon reservoirs and saline aquifers are critical targets for geological CO_2 storage. During CO_2 injection, the Joule-Thomson effect can potentially occur in the formations.

One crucial factor to consider during CCS is the thermal response of the reservoir, which is the Joule-Thomson cooling effect, which has great significance in the downstream and upstream petroleum industries.

The Joule-Thomson effect is a fluid's temperature change upon expansion in a steady flow process at constant enthalpy (Jamaloei & Asghari, 2015). In simple words, it is associated with the expansion of the injected gas when it spreads into a low-pressure reservoir.

Evaluating the Joule-Thomson cooling effect during CO_2 injection into depleted natural gas reservoirs is crucial. For example, if the Joule-Thomson effect is high, hydrates in the formation may form, affecting the well injectivity by lowering the reservoir permeability (Ziabakhsh-Ganji & Kooi, 2013).

When CO_2 is injected into the formation, the pressure in the near-wellbore area rapidly decreases as the gas expands into the reservoir. However, as the injected CO_2 reaches the warm formation, the CO_2 heats up, affecting its downhole conditions. Moreover, the downhole conditions can also be affected by other effects, such as a potential Joule-Thomson heating due to compression in the wellbore and two-phase evaporation/condensation processes over the length of the well (Jamaloei & Asghari, 2015).

According to Oldenburg, for low injection rates and permeabilities in the range expected in the Sacramento Valley (Rio Vista), California gas reservoir, the Joule-Thomson cooling effect has a minor effect (less than 4 °C). However, on the other hand, when the injection pressure is high and the CO2 is injected into a low-pressure reservoir, a Joule-Thomson cooling up to 20 °C is expected (Jamaloei & Asghari, 2015).

In depleted gas reservoirs with low pressure, the Joule-Thomson effect will be greatest for CO2 storage cases. In the case of saline aquifers at depths greater than 700m, where pressure is higher than 7 MPa, the Joule-Thomson effect is minor. This behavior can be seen in Figure 2.4.2.
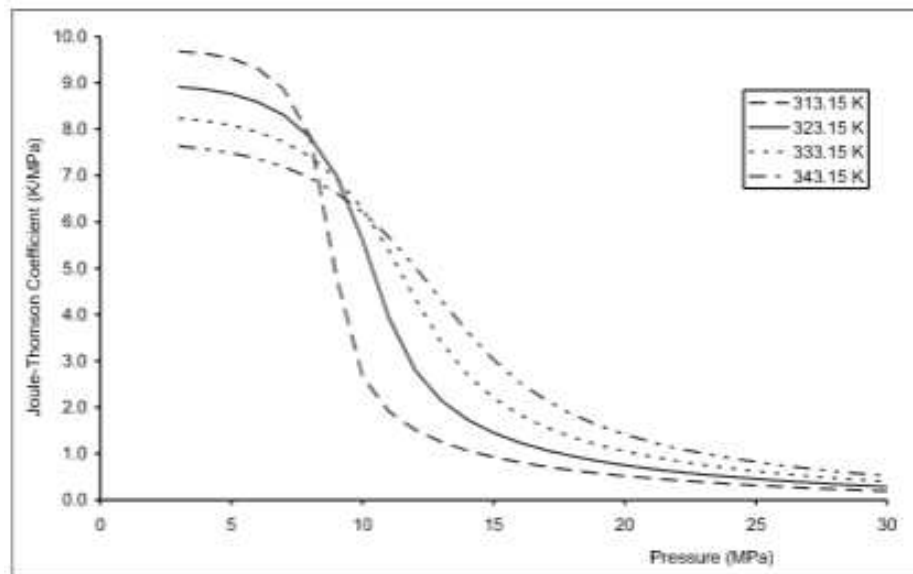
Figure 2.4.2 Joule-Thomson coefficient for CO2 as a function of pressure and temperature (data taken from NIST Chemistry Webbook) (André et al., 2009)

2.4.2 Hydrates formation

Gas hydrates consist of hydrogen-bonded water molecules encaging guest molecules, such as CO2 or CH4, which are formed at low temperatures and moderate pressures (Gauteplass et al., 2020). In other words, hydrates are solids composed of a mixture of water and gas molecules (Zatsepina & Pooladi-Darvish, 2011).

Hydrates formation is an exothermic process that releases heat to the reservoir. The kinetic reaction for CO2 and CH4 hydrates formation can be written as (Creusen, 2018):

$$CH_4(g) + nH_2O(aq) = CH_4.nH_2O(s) \pm heat \qquad (2.3.1)$$

$$CH_4(g) + nH_2O(aq) = CH_4.nH_2O(s) \pm heat \qquad (2.3.2)$$
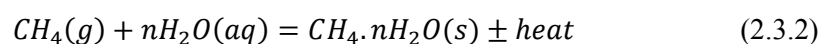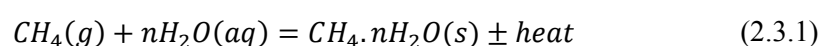
Gas hydrates formation in the porous media compromises the CO2 injectivity because it increases the flow resistance (friction) and local blockage. The pressure in the near-wellbore

area can be affected by sudden changes in CO2 injection rates, accelerating hydrate nucleation under certain thermodynamic conditions. Considerable pressure drops lead to Joule-Thomson cooling effect of CO2, causing hydrate nucleation or dry ice formation.

Mixed hydrates formation depends on the composition of the vapor phase. For example, Figure 2.4.3 shows the phase diagram for CH4-CO2 hydrates with 0, 20, 40, 60, 80, and 100% CO2 in the vapor phase (Zatsepina & Pooladi-Darvish, 2011).
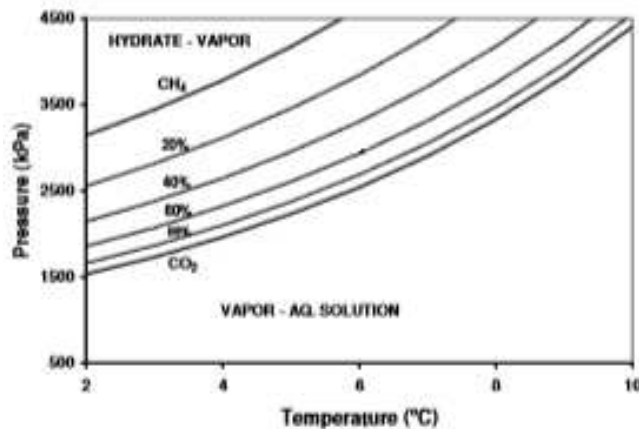

Figure 2.4.3 CH4-CO2 mixed hydrate phase diagram (Zatsepina & Pooladi-Darvish, 2011)

Figure 2.4.3, shows that at a fixed temperature, the mixed hydrate phase boundary spreads to lower pressures when increasing the CO2 fraction in the vapor phase.

Methanol or ethylene glycol and N2 are thermodynamic inhibitors used to dissociate gas hydrates. These inhibitors shift the phase equilibrium of hydrate formation and destabilize the hydrate structure at prevalent conditions (Gauteplass et al., 2020).

In case of a CO2-H2O system, the phase diagram for CO2 hydrates is shown in Figure 2.4.4. The blue and red curves represent the CO2 saturation line, and the hydrate formation conditions, respectively. The quadruple point is the point at which four phases coexist: CO2 in liquid, gas and hydrate phases, and an aqueous phase.

Co2 can exist in either liquid or gas state at low pressures and temperatures (subcritical conditions). And, if an adequate amount of water is present, at low temperatures, hydrates will form beyond the red line (Ramachandran et al., 2014).
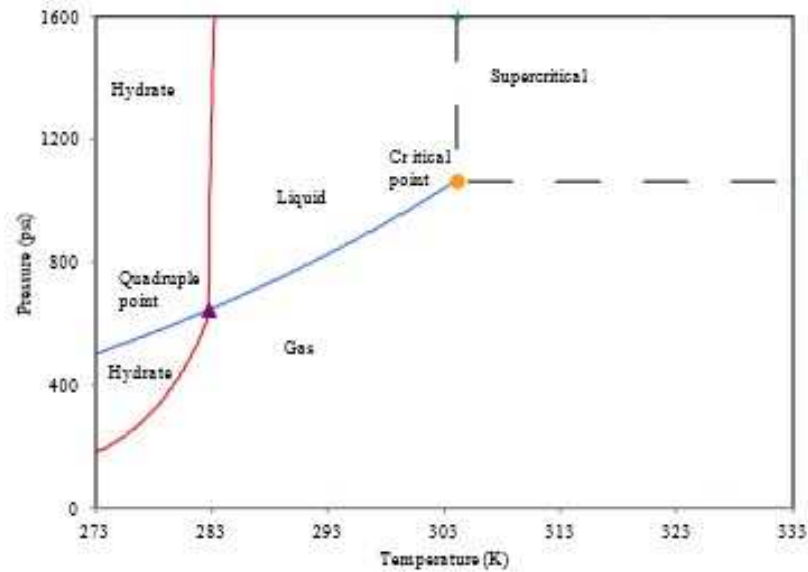
Figure 2.4.4 CO2-H2O hydrate phase diagram (edited from Ramachandran et al., 2014)

2.5   Transient effects in wellbore-reservoir modelling

Numerous models concerning the CO2 flow in the wellbore for geological long-term sequestration consider the flow in the steady-state condition or slow-changing flow where the inertia/storage effects in flow equations can be ignored or partially suppressed. However, in reality, the fluid flow is highly unsteady (transient flow), and, for instance, the equations concerning the thermal effects must be addressed (Paterson et al., 2010).

When injecting CO2 into the formation, it can undergo a phase transition along the wellbore, which restricts the numerical stability conditions along with the non-linear partial differential flow equations. A few models were developed to study instantly changing CO2 flow behaviors. However, these models simulate transient flow over terse times (in seconds or even a fraction of seconds). Wave propagation is considered in these models, but they would not be a practical approach for more prolonged transition problems (Lu & Connell, 2014).

Lu & Connell concluded that inertia and storage effects play a significant role in transient flow scenarios. Therefore, neglecting these effects may result in errors when simulating transient flow behavior. Moreover, in steady-state models, when the CO2 is in the two-phase state in the wellbore, the pressure and temperature profiles along the wellbore (Joule-Thomson coefficient) may no longer be suitable parameters. In addition, phase transition and heat transfer processes also play a significant role in the temperature profile of the fluid.

In addition, as the CO2 is flowing from the surface to the storage formation, depending on the pressure difference between the incoming fluid and wellhead pressure, the CO2 can experience drastic expansion and, thus, temperature drops, inducing the formation of hydrates (Revelation,

2017). Revelation stated that the analysis of start-up injection is crucial for predicting an optimum injection strategy for large-scale CO_2 sequestration.

2.6   Prior research studies

Research on geological CO_2 sequestration accelerated over the last 25 years (Creusen, 1970). As a result, numerous studies have been conducted on numerical modeling of CO_2 flow into geological formations, contributing to understanding the dynamic CO_2 flow behavior. For example, Hoteit et al. have demonstrated that the decoupled modeling is not accurate when describing the CO_2 flow behavior since it provides unrealistic results due to its incapability of capturing the transient effects occurring during the CO_2 vaporization process (Hoteit et al., 2019)

André et al. modeled CO_2 injection in its supercritical state into saline aquifers using the TOUGHREACT simulator and concluded that in an integrated modeling, thermal processes, such as CO_2 dissolution, Joule-Thomson effect govern both the fluid state and the chemical reactivity of the system (André et al., 2009).

Using the finite element numerical code CODE_BRIGHT, Vilarrasa et al. adopted a steady-state non-isothermal model approach from Lu and Connell. Vilarrasa et al. proposed CO_2 injection into its liquid state due to its advantages over supercritical CO_2 (Vilarrasa et al., 2013). They mentioned that this injection strategy is energetically advantageous, and a smaller compression at the wellhead is necessary due to the smaller compressibility of liquid CO_2. However, the dynamic evolution of the critical parameters, such as pressure and temperature (transient effects), should be considered since they can impact the long-term integrity and performance of CO_2.

Furthermore, in terms of choosing the most suitable coupled wellbore-reservoir simulator, Burachok et al. provided a functional comparison between different coupling solutions: COFLOW – integrated simulator, ECLIPSE Compositional (E300) – reservoir simulator, GEM – reservoir simulator, PROSPER – wellbore simulator, RESOLVE – integrated simulator, T2Well/ECO2N – integrated simulator, and Well Designer – wellbore simulator. Burachok et al. concluded that among these coupling solutions between wellbore and reservoir domains, COFLOW, T2Well/ECO2N, and tNavigator offer a fully implicit solver integration for CO_2 geological sequestration studies (Burachok et al., 2022).

Chapter 3

Simulation Model Setup and Benchmarking

The software used in this thesis is the transient wellbore-reservoir simulator T2WELL coupled with ECO2N EOS module, developed by the Lawrence Berkeley National Laboratory, which models the flow of CO2-H2O-NaCl mixtures either isothermally or non-isothermally (Pan et al., 2011). However, as a limitation of the ECO2N module, it can neither describe three-phase conditions (including both liquid and gaseous CO2-rich phase) nor phase change from liquid to gas or vice versa.

Input to T2Well simulator is provided as an open-format ASCII file. Unfortunately, the simulator has no pre- and post-processing capabilities, so neither the grid blocks nor the simulation results printed in the output file can be appreciated graphically.

Thus, the need arose to look for external software capable of reading and supporting either T2Well input or output files. In this thesis, Python was mainly used for both the automation of the input data (pre-processing tool) and graphical visualization of the results (post-processing tool).

3.1 Benchmarking of the CO2 Thermodynamic Properties

The T2Well simulator can model CO2-rich phase injection with no phase transition (ECO2N module) or phase transition (ECO2M). In order to know in which phase CO2 is being injected (liquid, gas, or supercritical), it is essential to know the thermodynamic properties of CO2, especially pressure and temperature. For example, if CO2 is over its critical pressure ($P_c = 73.9\ bar$) and temperature ($T_c = 31.04\ °C$), then CO2 is in the supercritical phase. In Figure 3.1.1, the phase diagram of CO2 can be observed.
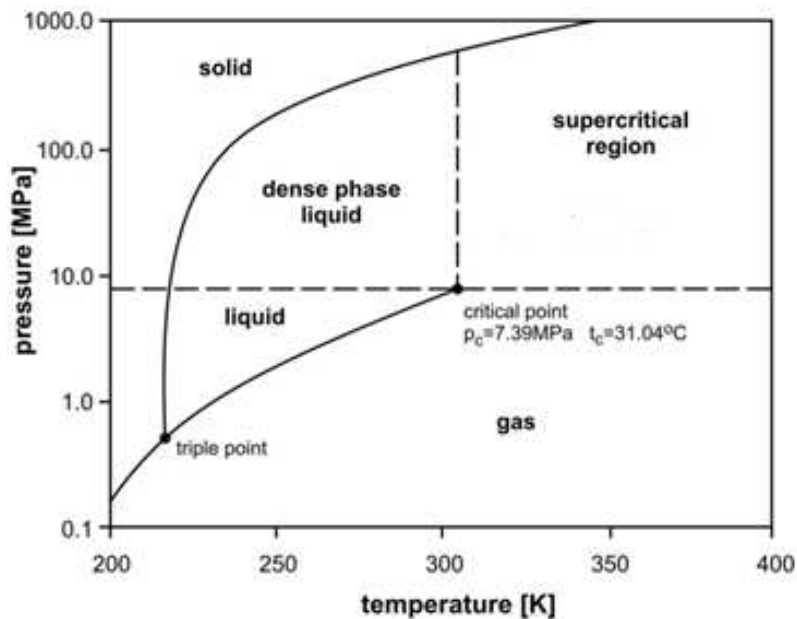
Figure 3.1.1 CO2 Phase Diagram (Witkowski et al., 2014)

The thermodynamic properties of CO2 are present in the ECO2N EOS module in a tabular form in a file named CO2TAB file. Properties of the CO2-rich phase are based on Altunin's correlations. Altunin's correlations were very accurate compared to experimental data and alternative PVT formulations, such as the Span and Wagner equation of state.

A benchmarking between Altunin's correlations and Span and Wagner EOS can be appreciated in Figure 3.1.2. The data are taken from the CO2TAB file and the REFPROP simulator used in NIST Chemistry Webbook.

From Figure 3.1.2, a good approximation between the CO2TAB file (T2WELL/ECO2N) and the Span and Wagner (NIST Chemistry Webbook) can be appreciated.

The property values data in the CO2TAB file were obtained by interpolation. The way CO2 properties were tabulated is shown in Figure 3.1.3, intentionally showing a coarse (T, P)-grid so that pertinent tabulation features may be better seen (Lawrence Berkeley National Laboratory, 2005).

In the ECO2N module, the CO2 temperature and pressure property data are in the range 3.04 °C≤T≤103.04 °C with ΔT=2 °C and 1 bar≤P≤600 bar with ΔP=4 bar in most cases.
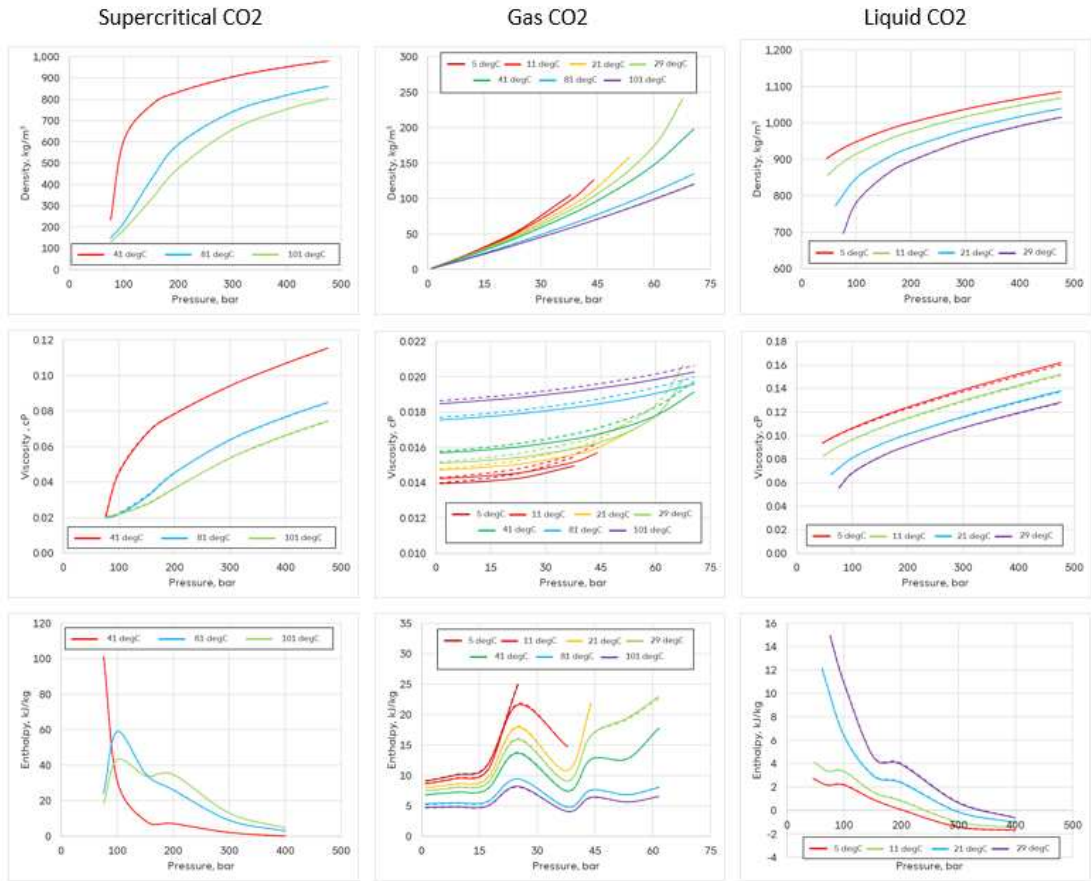
Figure 3.1.2 Thermodynamic properties comparison between T2WELL/ECO2N and NIST Chemistry Webbook (dashed lines – T2WELL/ECO2N, solid lines – NIST Chemistry Webbook) (Zamani et al. Evaluation of wellbore-reservoir response in coupled CO2 storage simulation (pre-printed))
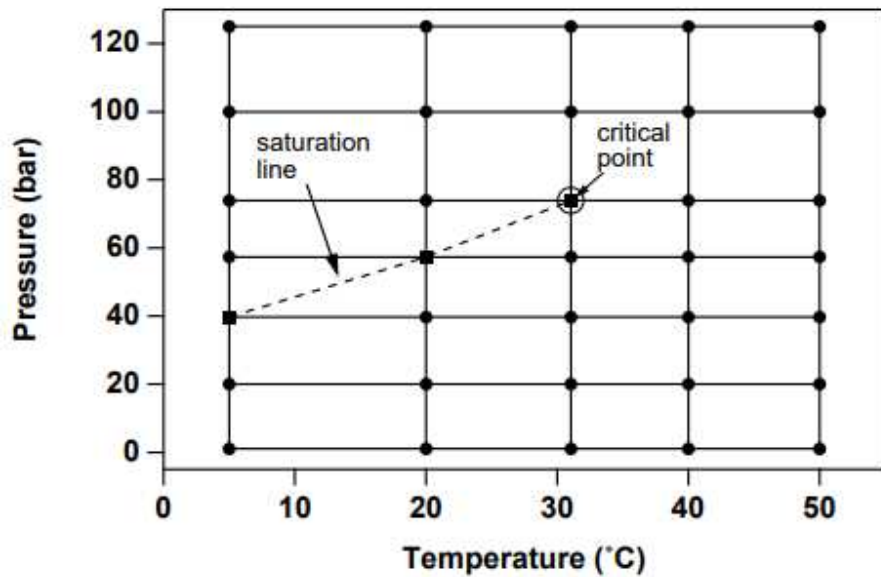
Figure 3.1.3 Schematic of the temperature-pressure tabulation of CO2 properties. The saturation line (dashed) is given by the diagonals of interpolation rectangles (Lawrence Berkeley National Laboratory, 2005)

3.2   Grid and conceptual model description

Hydrocarbon fields are usually associated with complex geological structures due to tectonic (faults) and structural (pinch-outs) elements, making the flow in wellbore-reservoir domain even more complicated.

Thus, gridding in reservoir simulation plays an important role. It allows the discretization of the system on which the fluid flow equations can be solved (Lake, 2006). Moreover, a grid is imposed on the reservoir to predict its behavior response to changes at the wellbore (Aziz, 1993). This thesis considers a two-dimensional radial model with a reservoir radius of 10 km. The bottom part of the storage reservoir is at 2500 m depth, consisting of a 50 m thick permeable formation with porosity and permeability equal to $\emptyset = 0.2 \; and \; k = 100 \; mD$, respectively, overlaid by a 50 m caprock with a porosity and permeability equal to $\emptyset = 0.05 \; and \; k = 0.001 \; mD$, respectively. Both formation and caprock are considered homogeneous domains, thus the ratio of horizontal to vertical permeability is set to 1.

Both caprock and formation storage are initially fully saturated with brine – 5% NaCl and 95% H2O. In the case of the wellbore, it is fully saturated with water since salt water can lead to corrosion of the pipe. In real case, instead of water, cushion gas is injected within the wellbore to prevent water-CO2 contact to avoid possible corrosion (Zamani et al., 2023). Nevertheless, T2Well cannot model this procedure since it only handles CO2-H2O-NaCl mixtures.

The wellbore and reservoir system are initially in equilibrium considering a hydrostatic pressure gradient equal to 9810 Pa/m and a geothermal gradient of 0.01 °C/m, resulting in storage formation pressure and temperature equal to 250 MPa and 60 °C. Since the ECO2N module cannot handle phase transition from gas to liquid or vice versa, the wellhead temperature is set to be constant and equal to 35 °C for the gas CO2 injection case and 40 °C for the supercritical case.

The wellbore is considered at the leftmost side of a model extended from the surface to the bottom part of the reservoir. The internal wellbore diameter is 6 in (about 15 cm), connected to the formation between 2450 and 2500 m. A semi-analytical approach is considered for heat exchange between the wellbore and the surrounding area.
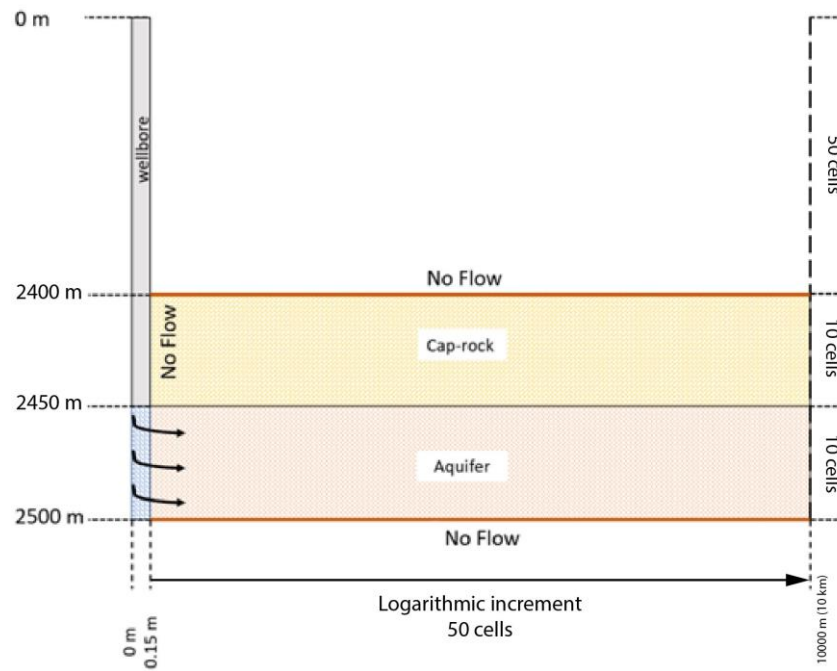
Figure 3.2.1 Model description (edited from Zamani N. et al., 2023 – preprinted)
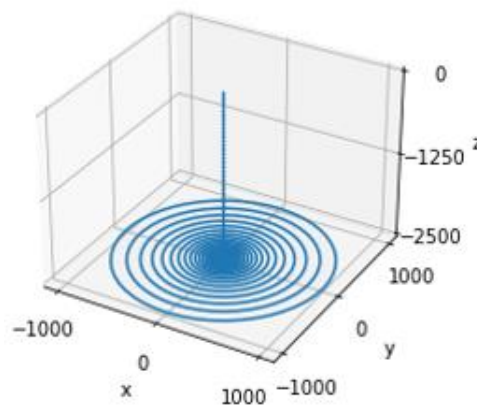

Figure 3.2.2 3-D wellbore-caprock-reservoir discretization

As seen from Figure 3.2.1, the wellbore is discretized into 50 cells of uniform thickness equal to 50 m. Both porous media and caprock are discretized radially with variable cell size (logarithmic increment) so that the cell is finer near the wellbore and gradually becomes coarser towards the outer boundary. Both caprock and reservoir are divided into 10 layers of 5m thickness each. This is done in order to capture the gravity effect during CO2 propagation in the formation.

At the rightmost side of the reservoir and caprock, Dirichlet boundary condition is used for a huge volume grid to keep the pressure and temperature constant at initial pressure and geothermal gradients. The injection conditions at the wellhead control the boundary condition at the wellbore, as seen in Figure 3.2.3.
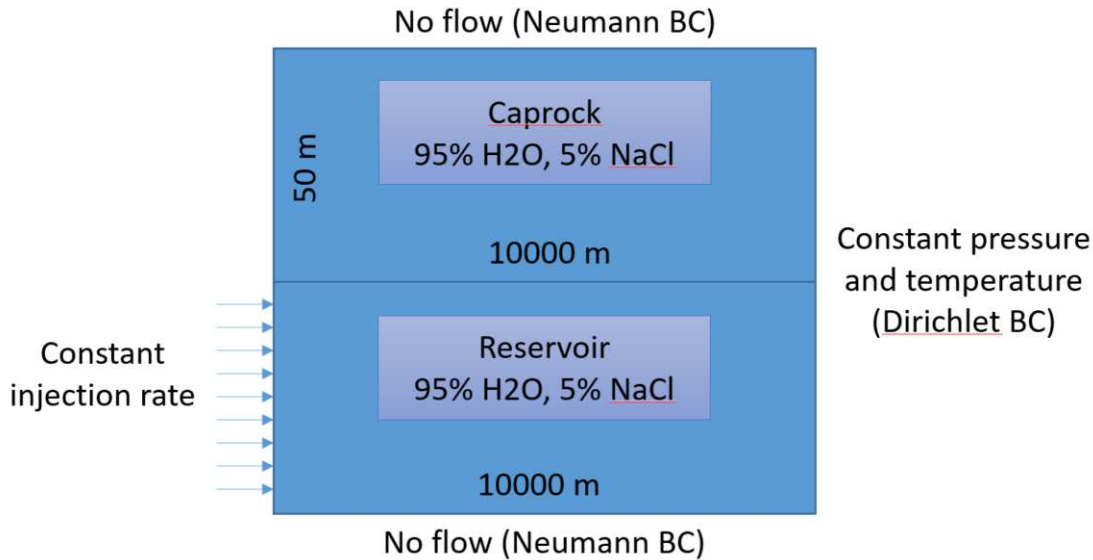
Figure 3.2.3 Model boundary conditions

For the gas CO2 injection case, the wellhead pressure is equal to 65 bar, while for the supercritical CO2 case, the pressure at the wellhead is 80 bar. Therefore, for both cases to be comparable, the mass rate is constant during the simulation time and equal to 1 MMtonn/year (about 32 kg/s).

The Van Genuchten-Mualem model (Genuchten, 1980; Mualem, 1976) is used for capillary pressure and relative permeability in the formation, and Corey's model for relative permeability in the caprock. More details about the Van Genuchten-Mualem and Corey's model can be found in the TOUGH2 User's Guide, Version 2 manual (Lawrence Berkeley National Laboratory, 1999).

3.3   Model parameters

Once the wellbore and formation are discretized, the model parameters of the system are required to be defined in the T2Well input file. These parameters used for the model are shown in Table 3.3.1,

Table 3.3.2, Table 3.3.3, and Table 3.3.4

Table 3.3.1 Model formation properties

Formation Properties	Values	
	Storage (aquifer)	Caprock
Compressibility, 1/Pa	8.5e-10	
Density, kg/m^3	2600	
Heat conductivity, W/(m*°C)	1.5	
Thickness, m	50	

Porosity	0.2	
Permeability, mD	100	0.001
Specific heat J/(kg*°C)	874	

Table 3.3.2 Model transport parameters

Transport Parameters	Values	
	Storage (aquifer)	**Caprock**
Capillary pressure	Van Genuchten model	Corey's model
	$\lambda = 0.7, S_{lr} = 0.3$ $S_{ls} = 0.95, S_{gr} = 0.05$	$S_{lr} = 0.3, S_{gr} = 0.05$
Relative permeability	Van Genuchten model	
	$\lambda = 0.457, S_{lr} = 0.36$ $1/P_0 = 8e^{-5}$ $P_{max} = 1e^7, S_{ls} = 0.999$	$\lambda = 0.25, S_{lr} = 0.2$ $1/P_0 = 1e^{-5}$ $P_{max} = 1e^{11}, S_{ls} = 1$

Table 3.3.3 Model wellbore properties

Wellbore Properties	Values
Depth, m	2500
Internal diameter, in	6

Table 3.3.4 Model general properties

General Properties	Values	
	Gas CO2	Supercritical CO2
Injection mass rate, kg/s	32	
NaCl mass fraction	0.05	
Reservoir temperature, °C	60	
Reservoir pressure, bar	244	
Wellhead temperature, °C	35	40
Wellhead pressure, bar	65	85
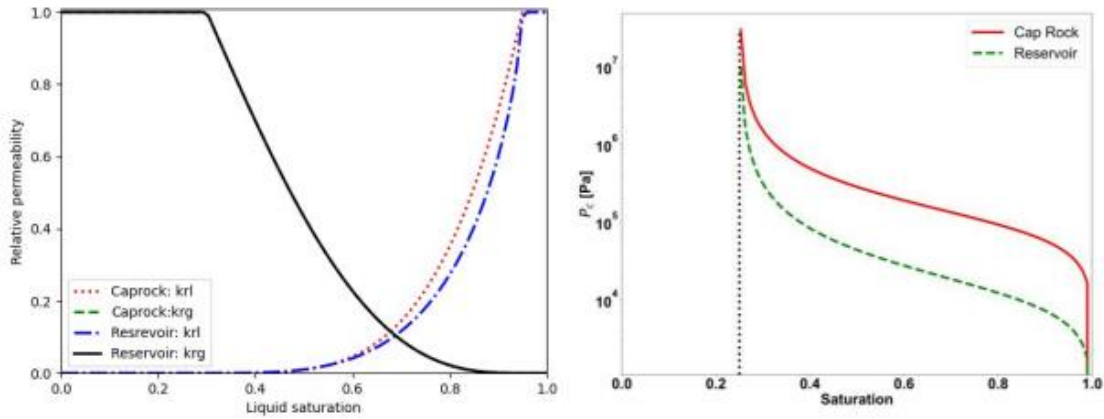
Figure 3.3.1 Relative permeability and capillary pressure used for the caprock and reservoir (Zamani et al., 2023)

To have a visual understanding of the fluid phase at initial stage (before CO2 injection), Figure 3.3.2 shows CO2-H2O phase diagram. The brown and aqua lines represent the melting and saturation curves of CO2 and water, respectively. The dark violet line represents the hydrostatic initial conditions (before injection starts) used in the model explained above. The grey points represent the CO2 injection conditions – 65 bar, 35 °C for the CO2 gas case and 80 bar, 40 °C for the supercritical case.
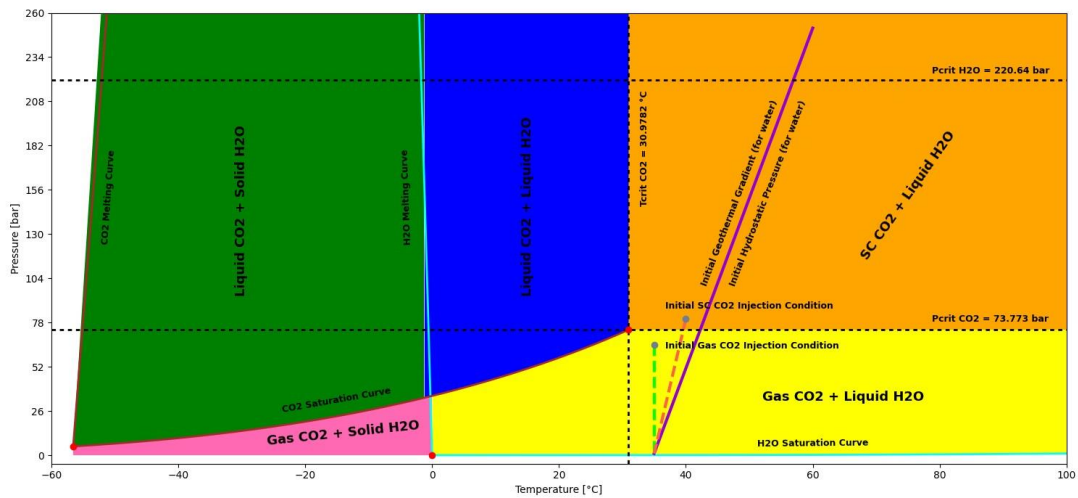
Figure 3.3.2 CO2-H2O phase diagram

3.4   Case description

This Master's thesis focuses on the multiphase (water-NaCl-CO2 mixture) fluid flow in a coupled wellbore-reservoir system. A conceptual model is used to study the CO2 behavior along the wellbore, phase transition (from gas to supercritical or vice versa), pressure and temperature profiles, and CO2, pressure, and thermal fronts along the storage formation.

Two cases will be evaluated: one with CO2 injection in its supercritical state (80 bar and 40 °C at the wellhead) and the second with CO2 in its gas phase (65 bar and 35 °C at the wellhead). For both cases, CO2 will be continuously injected from the surface to the subsurface for 5 years at a constant mass rate equal to 1MMtonn/year.

The CO2 propagation within the formation is affected by the different thermal processes the CO2 experiences when traveling 2500 m from the surface to the formation. For example, since the injected CO2 is colder than the formation, a cooling effect (Joule-Thomson effect) can be observed in the near-wellbore area, which, in some cases, can lead to hydrates formation depending on the injection conditions.

Chapter 4

Results and Discussion

4.1 CO2 flow behavior in the wellbore

In order to better capture the transient effects, Figure 4.1.1, Figure 4.1.2 and Figure 4.1.3 show the CO2 evolution, pressure, and temperature propagation over the first three hours of simulation, respectively, after CO2 injection started along the wellbore. The vertical dashed lines represent the filling time, i.e., the time required in which the water in the wellbore is fully displaced by the injected CO2 into the formation storage.
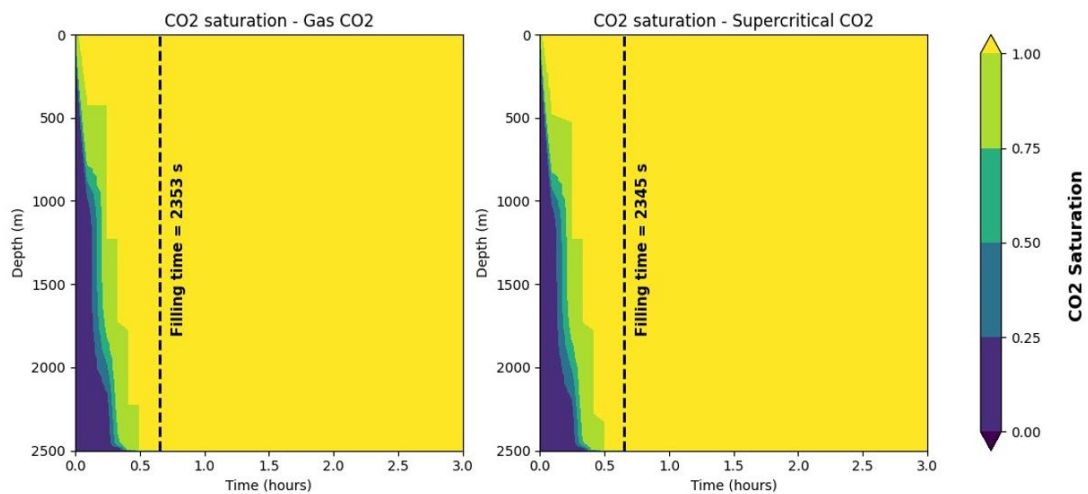
Figure 4.1.1 CO2 saturation along the wellbore
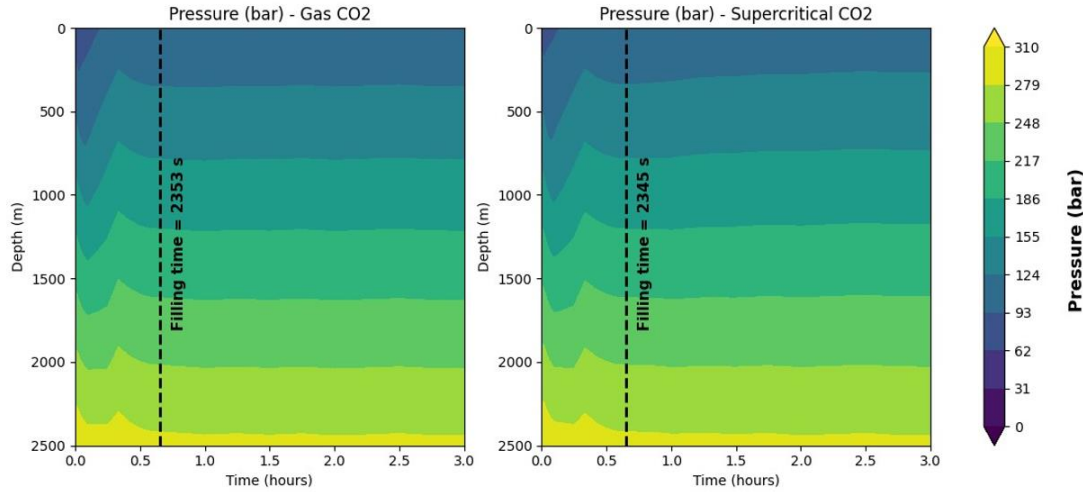
Figure 4.1.2 Pressure propagation along the wellbore
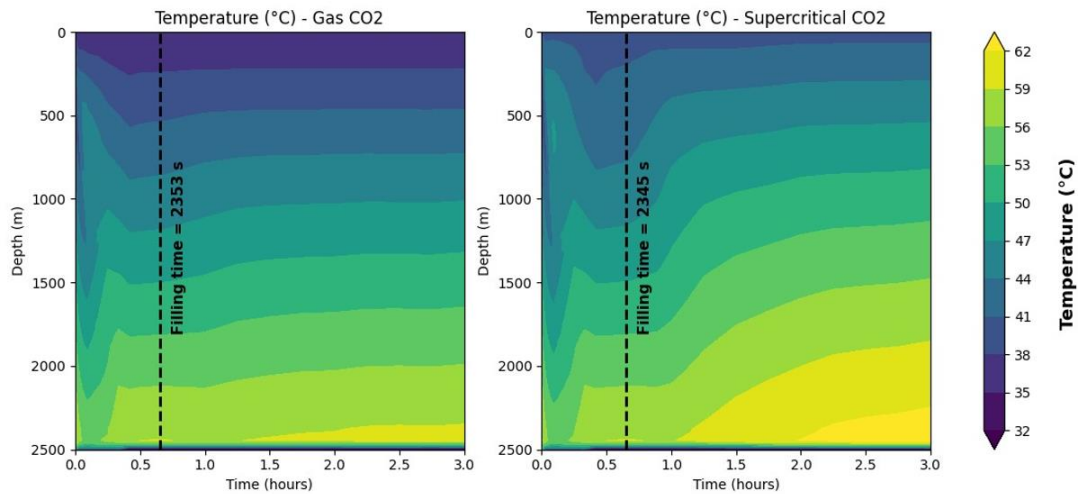
Figure 4.1.3 Temperature propagation along the wellbore

In these figures, three regions can be appreciated: i) initial state, ii) transient state, and iii) steady state. The first region is at the initial time step (before CO2 injection starts), in which the wellbore is fully filled with water, and pressure and temperature distribution follows the hydrostatic pressure and a geothermal gradient, respectively. The second region is when injection starts and both CO2 and water flows together (multiphase flow). And, the third region is when the water was fully displaced by the injected CO2, thus, only CO2 is flowing along the wellbore.

In Figure 4.1.2, at the second stage, a decrease in pressure for a short period of time, about 330 seconds (ca. 5.5 minutes) and 280 seconds (ca. 4.7 minutes) for the supercritical and gas CO2 case, respectively, can be noticed, accompanied with a pressure build-up. This behavior can be related to the higher flow resistance within the porous media compared to the wellbore (Nematollah et. al, 2023).

During geological sequestration, the heat transfer mechanism is mainly controlled by convection – since the injected CO2 is usually colder than its surroundings, it gains heat when flowing through the wellbore (Lu & Connell, 2014). However, In Figure 4.1.3, this opposite behavior can be seen, meaning that the wellbore temperature does not decrease over time. This effect is related to the rock heat conductivity, which is not high enough to effectively transfer heat from the wellbore to its surrounding area.

Moreover, since the CO2 is colder (35 °C and 40 °C for the gas and supercritical case, respectively) than the reservoir (60 °C), it cools down the formation (JT effect), leading to a decrease in temperature in the wellbore cells where the perforations are located, as seen from Figure 4.1.3.

Furthermore, it does not matter in which state the CO2 is being injected, it will reach the reservoir (top layer) in the supercritical phase, as seen from Figure 4.1.3, which matches that as stated by Vilarrasa et al. They showed that injecting liquid, gas, or supercritical CO2 into deep saline aquifers will reach the reservoir at supercritical condition at the steady state condition (Vilarrasa et al., 2013).

As a complement to Figure 4.1.2 and Figure 4.1.3, Figure 4.1.4 and Figure 4.1.5 better show the pressure and temperature variation along the wellbore after CO2 injection started, indicating at which depth phase transition occurs. Phase transition for the gas CO2 injection can be appreciated twice – from gas to supercritical, and from supercritical to liquid – while for the supercritical CO2 case, the fluid changes its state once: from supercritical to liquid.

In case first case, the CO2 changes from gas to supercritical at the wellhead as soon as the injection starts due to the pressure increment caused by the injection process. (H = 0 m, t = 140 s). The second transition – from supercritical to liquid – occurs at the perforation levels (H = 2450 m, t = 2100 s). As the figure shows, the temperature significantly decreases due to the JT effect, as explained above. For the supercritical CO2 case, the transition is from supercritical to liquid due to the JT effect (H = 2450 m, t = 2100 s).

From Figure 4.1.4 and Figure 4.1.5 it can be noticed that, for both cases, the pressure rapidly deviated from the initial hydrostatic condition, while, in contrast, the temperature deviates slowly from the initial geothermal gradient due to thermal process the injected CO2 experiences when flowing to the reservoir.

Moreover, during the first hours of simulation, the temperature presents a "zigzag" behavior – increases to a depth around 400 m, then it starts decreasing until 1000 m, and finally starts increasing again until reaching the perforation levels (H = 2450 m), from which the CO2 starts cooling again.

Figure 4.1.4 and Figure 4.1.5 supports what said above for Figure 4.1.2 and Figure 4.1.3, and results are consistent with previous works (Biselli et al., 2011; Lu & Connell, 2014)
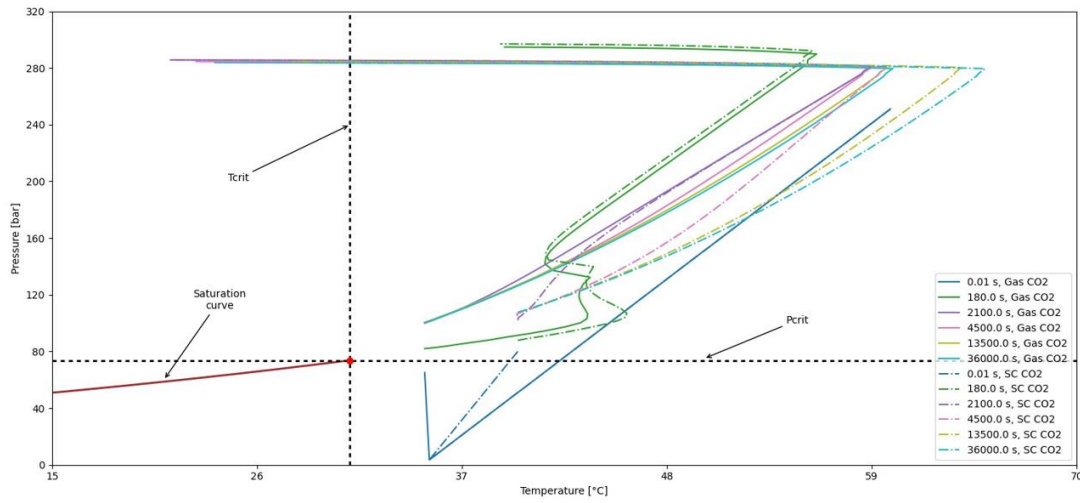

Figure 4.1.4 PT evolution along the wellbore for the gas (solid) and supercritical (dashdot) CO2 injection cases
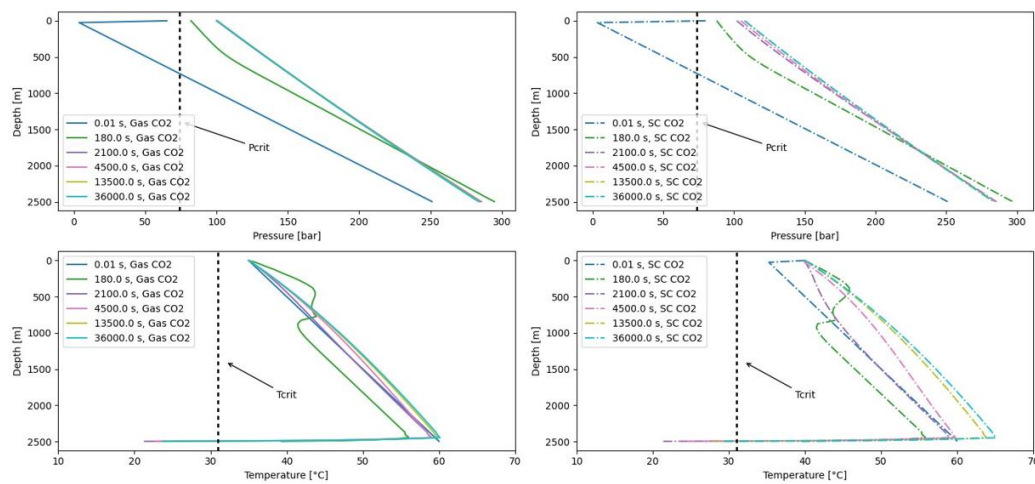

Figure 4.1.5 Pressure (top) and temperature (bottom) profile along the wellbore for the gas (left) and supercritical (right) CO2 injection cases

However, the temperature drop at the perforations level is abnormal. Usually, such a high JT-effect usually happens in the temperature range of 350 K – 500 K and pressures up to 7 MPa approximately, as seen from the JT inversion temperature curve in Figure 4.1.6. The plot was generated in Matlab using data from the NIST Chemistry Webbook.
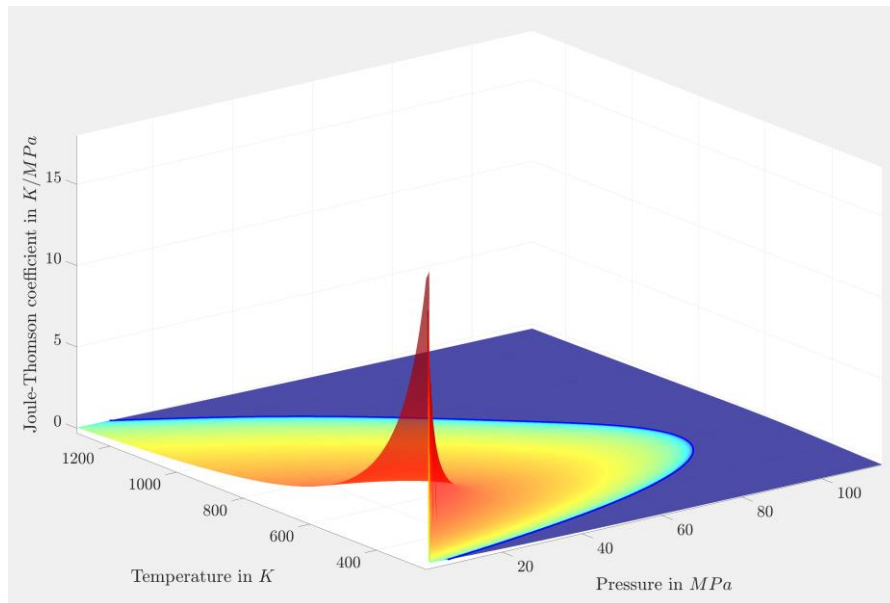
Figure 4.1.6 Joule-Thomson temperature inversion curve

The abnormal drastic temperature drop shown in Figure 4.1.5 can be related to the semi-analytical approach for the heat transfer between the wellbore and the surrounding area. The semi-analytical approach was presented by Yingqi et al. to simplify the heat transfer mechanism between the wellbore and the surrounding area in order to improve the computational efficiency. This approach considers only the discretization of the wellbore, and it is assumed that the vertical heat transfer within the formation is small and that the formation above the reservoir has very low permeability in order to ignore the convective heat transport (Yingqi et al, 2011).

Even though the accuracy of the semi-analytical approach is accurate compared to the full-scaled discretization model of rock formation, as shown by Yingqi et al., this heat transfer simplified approach is not sufficient since convection heat transfer of CO2 in tubing and the impacts of thermal convection of fluids in annulus must be analyzed in order to understand and prevent formation failure (Ruan et al., 2013).

Moreover, Jiang et al. compared the full-field model with rock formation and the simplified model, and showed that the bottomhole is about 20 °C less when using the simplified heat flux model at low rates, presenting an error of roughly 25%, as seen in Figure 4.1.7.
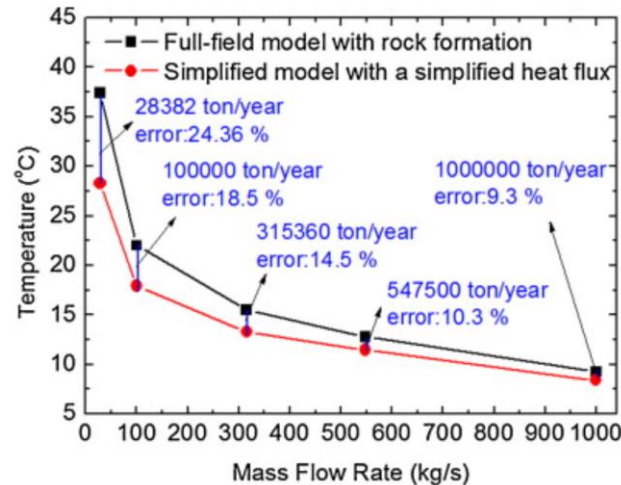
Figure 4.1.7 Bottomhole temperature of CO2 at different mass flow rates in both the full-field model with rock formation and the simplified model after 10 days (Jiang et al., 2014)

4.2   CO2 flow behavior in the storage formation

Ensuring safe CO2 geological sequestration relies on the CO2 plume evolution along the subsurface and presents significant challenges. Thus, tracking plume characteristics, as well as pressure and temperature wave propagation along the formation storage is crucial for the integrity of sequestration operations in saline aquifers (Zapata et al., 2022).

Injection of dry CO2 leads to immiscible displacement of resident aqueous phase, and to water dissolution into the flowing CO2. In one space dimension, two fronts are present: 1) two-phase conditions (displacement front), and 2) a dry-out front, which is accompanied by solid precipitation, reducing porosity, permeability, and injectivity (Pruess, 2009).

Figure 4.2.2 shows how the pressure changes along the caprock and storage formation in the near-wellbore area at different time steps – after 2, 4 6, and 8 years for both CO2 gas and supercritical cases. It can be seen that the pressure significantly increases.

After 2 years of continuous CO2 injection, right next to the wellbore, at the top reservoir layer, the pressure increases from 246 to 278 and 279 bar for the supercritical and gas case, respectively. And at the bottom layer, it increases from 251 to 282 bar for both cases. This high-pressure buildup in the storage formation is related to the relative high amount of CO2 injected into the reservoir (1 MMtonn/year). However, with time, this pressure increment decreases.

When moving further from the wellbore, it can be also seen that the pressure continuously decreases further from the wellbore along the radial direction to its initial value for both cases (before CO2 is injected), as seen from Figure 4.1.2.

In addition, from Figure 4.2.2 it can be also noticed that the pressure waves not only propagate along the reservoir, but also through the caprock, meaning that CO_2 escapes into the caprock. The pressure wave propagates anisotropically from the storage formation to the caprock – with a different slope in the reservoir than in the caprock. This is related to the different permeability – 0.001 mD for the caprock and 100 mD for the storage formation. This anisotropic pressure propagation can be better seen in Figure 4.2.2.
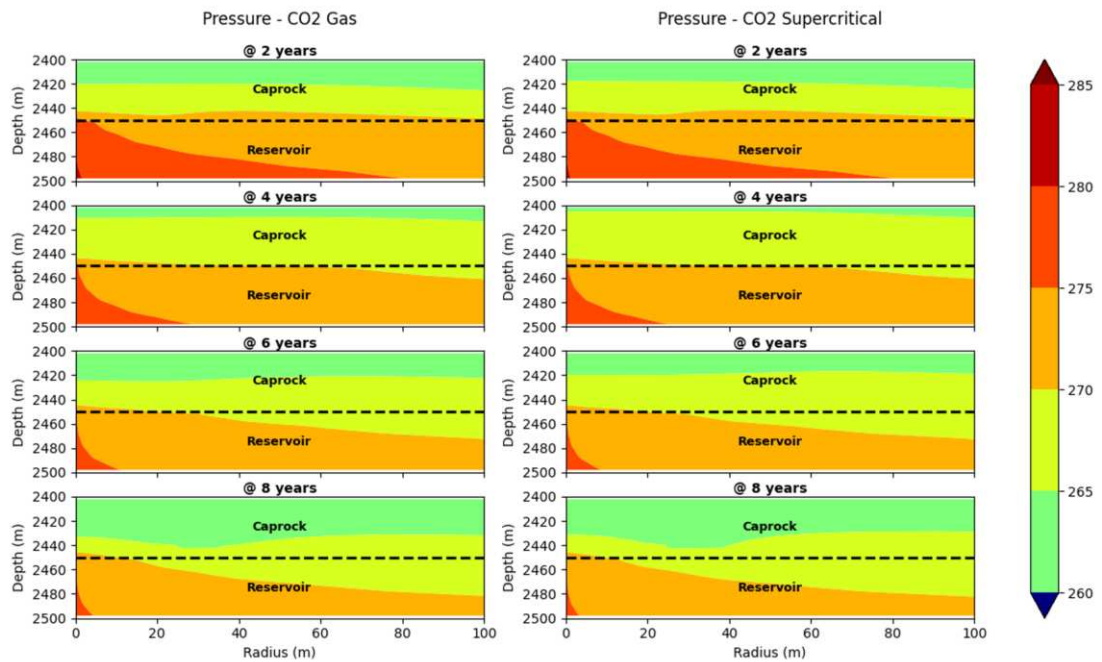
Figure 4.2.1 Radial pressure distribution along the caprock and reservoir in the near-wellbore area
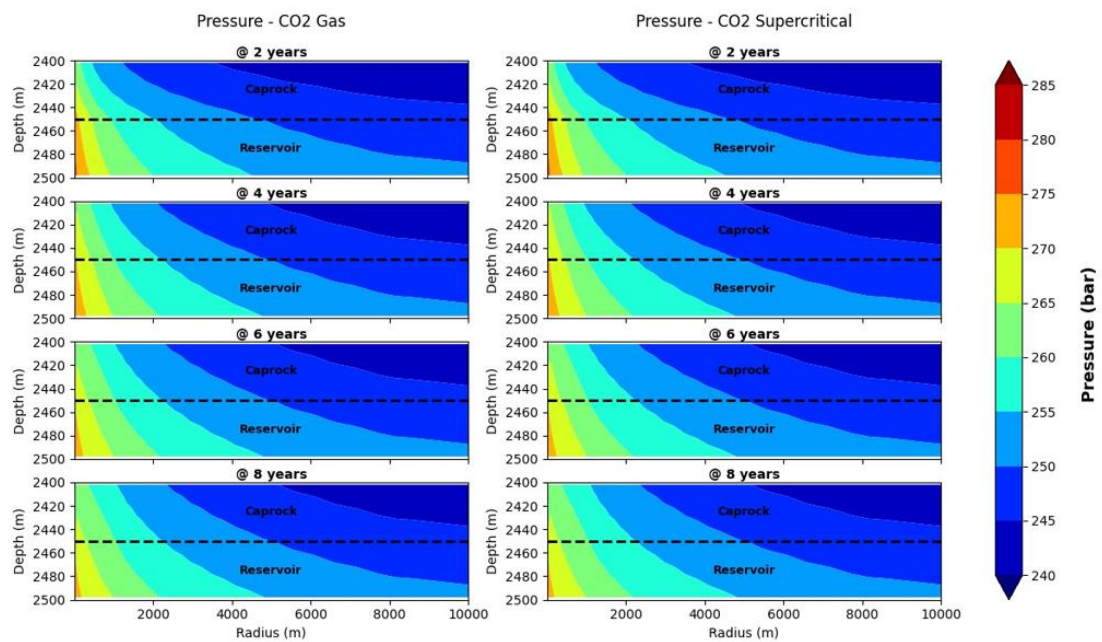
Figure 4.2.2 Radial pressure distribution along the whole caprock and reservoir

Figure 4.2.3 shows how the temperature change along the caprock and storage formation in the near-wellbore area at different time steps – after 2, 4 6, and 8 years for both CO2 gas and supercritical cases.

As colder CO2 is injected into a warmer reservoir, it cools down the storage formation in the near wellbore area. This behavior is related to the JT effect, which causes the gas to expand, leading to a decrease in pressure. Oldenburg stated that the JT effect will be greatest when injecting CO2 into highly depleted gas fields.

The highest temperature decrease occur at the bottom layer of the storage formation. For the CO2 gas, the temperature decreased from 60 to 24 °C, while for the supercritical CO2 case, it decreased to 31 °C, meaning that the cooling effect is higher when injecting CO2 in its gas phase at the surface. This is related to the heat capacity of supercritical CO2, being higher than the gaseous state. This means that supercritical CO2 can carry heat energy within the reservoir more efficient than the gaseous CO2.

In addition, from Figure 4.2.3, it can be also seen that the caprock and the top of the reservoir heats up much more when injecting supercritical CO2 than gaseous CO2. As mentioned previously, due to the semi-analytical heat transfer approach in the wellbore, the convective heat flux is ignored, causing the wellbore temperature to rise with time to a value higher than the initial reservoir temperature at the lower part of the wellbore.
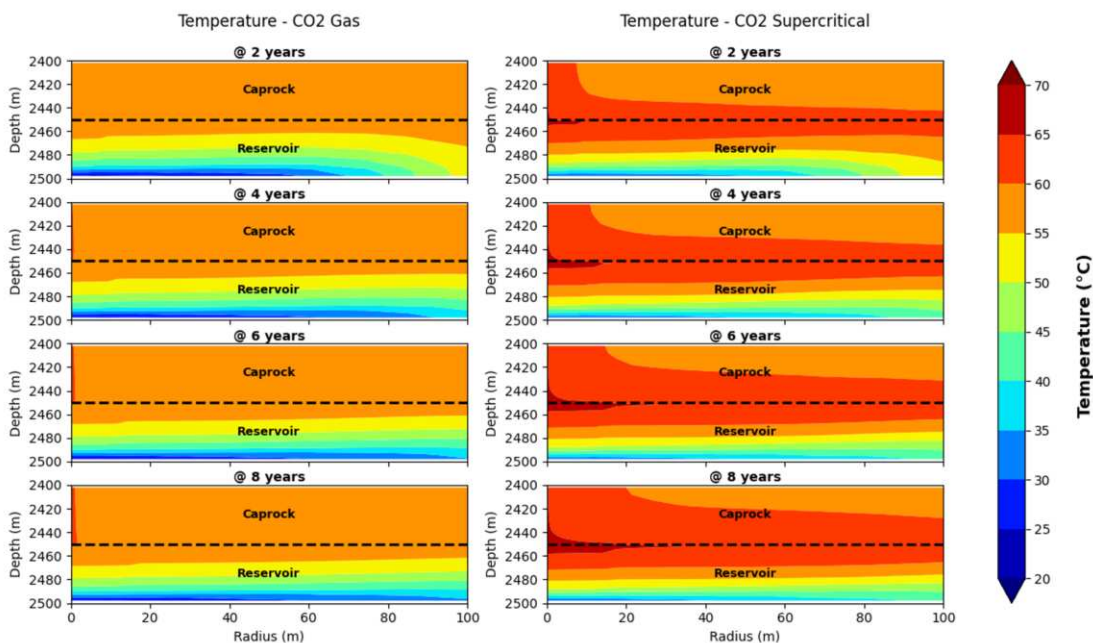
Figure 4.2.3 Radial temperature distribution along the caprock and reservoir in the near-wellbore area

Moreover, since the wellhead injection temperature is higher for the supercritical case, it will cause a higher bottomhole temperature, as described by Sokama-Neuyam et al., 2022, who showed the effect of injection temperature on CO2 injectivity. Thus, for these reasons, more heat is transferred from the wellbore to the caprock and the top of the reservoir for the supercritical case.

As seen from Figure 4.2.4, for both cases, the JT-effect reaches about 200 m away from the wellbore after 8 years of continuous injection. However, it reaches a higher vertical distance from the bottom reservoir layer for the gas CO2. After the cooling behavior, the temperature starts gradually increasing, exceeding the initial reservoir temperature due to CO2 dissolution, and then decreases until the initial reservoir temperature.

Furthermore, since the thermal front moves into the reservoir as a function of the imposed flow rate, the cooling effects reaches a higher distance from the wellbore with time. Different studies have shown that, in case of CO2 injection into deep saline aquifers for geological sequestration, the CO2 dissolution in brine produces a local temperature increment, as stated by André et al., 2010 and Bielinski et al., 2008.

After 2 years of continuous CO2 injection, the temperature at the bottom of the reservoir increases to a maximum value of 60.36 °C for the gas CO2 case, and to 60.76 °C for the supercritical CO2 case, while for the end of the whole simulation time (8 years), the temperature increased to 60.67 °C for both cases, as seen from Figure 4.2.4.
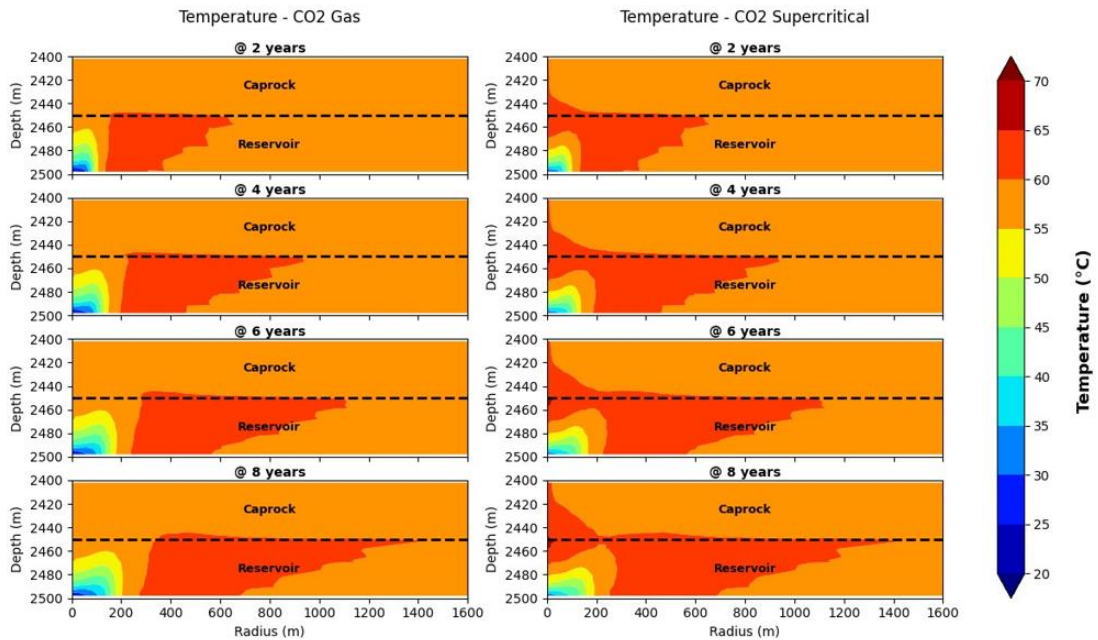
Figure 4.2.4 Radial temperature distribution along the caprock and reservoir

On the other hand, high CO2 injection mass rate leads to the formation of a two-phase system – supercritical CO2 and brine (for both CO2 gas and supercritical injection cases, the CO2 reaches the reservoir in its supercritical state as explained before). Depending on pressure and temperature conditions, part of the CO2 dissolves in the water whereas the remaining CO2 stays in its own supercritical state (André et al., 2010).

Figure 4.2.6 shows the extension of the CO2 and the position of the two-phase (CO2 front) along the caprock and storage formation in the near-wellbore area. It can be seen that after 2 years of continuous CO2 injection, desiccation (dry-out zone) occurs in the proximity of the injection well, reaching a distance of about 7 m away from the wellbore for both cases, followed by a two-phase system (supercritical CO2 – saline water) in the storage formation.

Moreover, it can be visually seen that what was explained above. Since the injection temperature is lower than the host storage formation, the caprock fractures, allowing the CO2 to escape from the reservoir, reaching the two last bottom layers after 2 years of simulation and three bottom layers after the whole simulation time (8 years) for both cases.

Caprock failure during CO2 injection can be induced by the injection temperature. According to numerous articles (Gor & Prévost, 2013; Yu et al., 2013; Vilarrasa et al. 2015) when the temperature at which the CO2 is injected is lower than the storage formation's, the thermal stresses exceed that tensile strength.
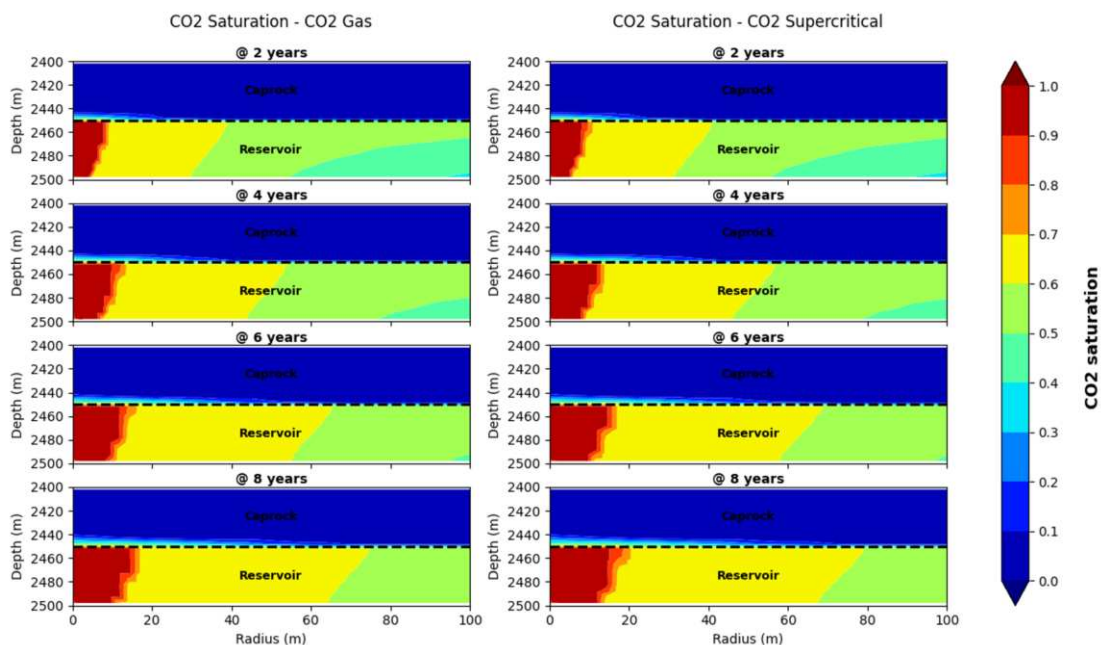
Figure 4.2.5 CO2 front along the caprock and reservoir in the near-wellbore area

In addition to the tensile strength effect, migration of CO2 into the caprock can be also caused when the CO2 fluid pressure in the reservoir exceeds the capillary entry pressure – breakthrough (threshold) pressure. When exceeding this breakthrough pressure, the continuous flow of the non-wetting fluid along the pore system, the CO2 can escape from the upper boundary of the storage formation (Busch et al., 2010; Kivi et al., 2021).

Also, the effect of gravity plays a role during CO2 injection. Due to the density difference, the injected CO2 reaches a higher distance at the top layer than its bottom neighboring layer. At the end of the simulation time (8 years), the two-phase system reaches a radius of about 1060 m at the top reservoir layer and 880 m at the bottom for both case scenarios, as seen from Figure 4.2.5 and Figure 4.2.6.
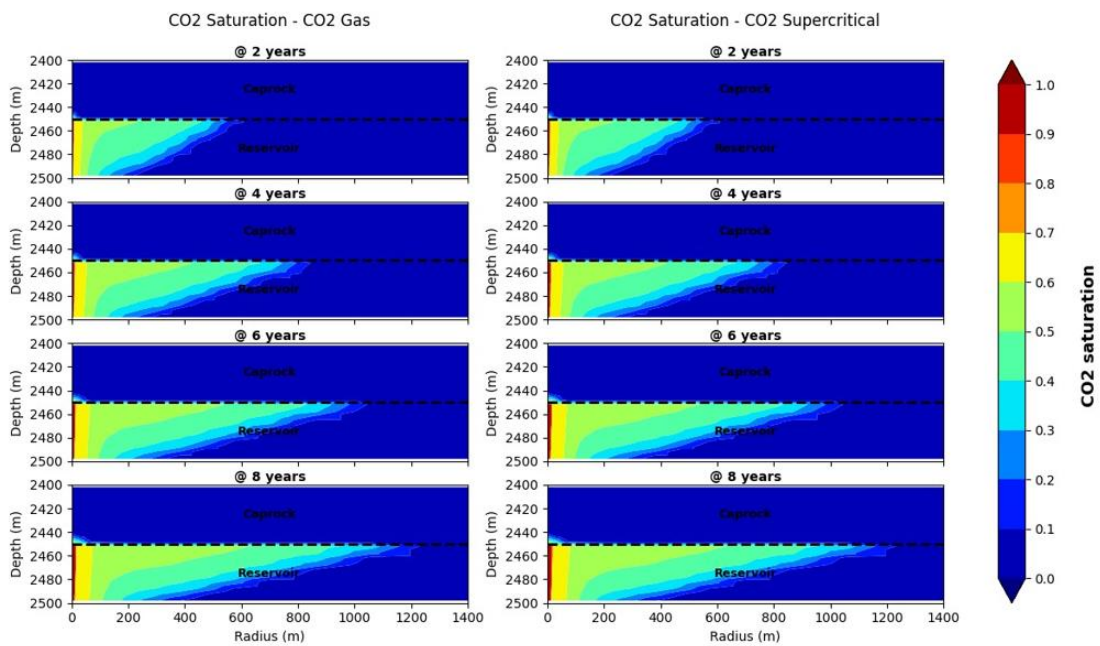
Figure 4.2.6 CO2 front along the caprock and reservoir

Figure 4.2.7 shows the solid saturation in the storage formation. As seen from the figure, salt precipitation occurs in the near wellbore area – within 7.6 m and 4 m at the top and bottom layer, respectively for the CO2 gas case, and 9.4 m and 5 m at the top and bottom layer, respectively for the CO2 supercritical case after 2 years of continuous injection.

During CO2 injection, when multiphase fluid flow forms in the storage formation, the water phase constantly evaporates and diffuses into CO2 due to the mass transfer between these two fluids, resulting in the precipitation of the dissolved salt. The precipitated salt migrates downwards and accumulates at the bottom of the reservoir due to the drag force (Cui et al., 2023).

Even though the aquifer's salinity was set to a low value, severe salt precipitation may occur in the near-wellbore area when the reservoir permeability is low (Cui et al., 2023), as shown in Figure 4.2.7. It can be also seen that the extent of salt precipitation increases over time. Moreover, the amount of salt precipitation is higher for the CO_2 gas case, leading to a less porosity reduction than the supercritical case. Thus, it will require a higher pressure at the wellhead (about 7 bar) to displace the brine in the aquifer, as seen in Figure 4.1.2.
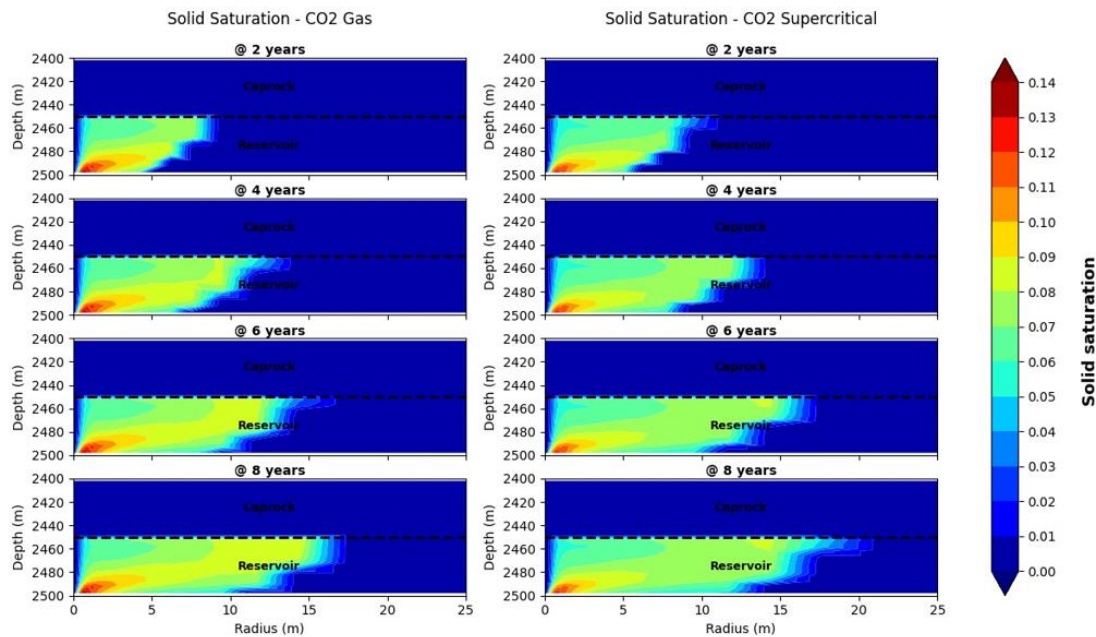
Figure 4.2.7 Solid saturation along the caprock and reservoir

In addition, since the CO_2 saturation is not significant in the caprock (no dry-out zone forms) as seen from Figure 4.2.5 and Figure 4.2.6, salt precipitation in the proximity of the well does not occur, as seen from Figure 4.2.7. Moreover, as mentioned previously, salt precipitation threatens the CO_2 injectivity by significantly reducing the reservoir porosity and permeability due to local blockage in the near-wellbore area. Thus, it is imperative to reduce salt precipitation.

One method to reduce salt precipitation in the proximity of the well, a low-salinity water slug can be injected prior to CO_2 injection in order to prevent direct contact of CO_2 and the formation water. This way the water evaporation will be minimized, and local salt precipitation can be avoided (Cui et al., 2023).

However, if salt was already precipitated in the near-wellbore region, another method to reduce the salt precipitation is by injecting a low-salinity water slug in order to dissolve the precipitated salt and, thus, increase the reservoir permeability (Cui et al., 2023). A third method (and probably the most effective) is to inject CO_2-H_2O mixture to reduce or even eliminate the formation water evaporation (Cui et al., 2023).

Chapter 5

Conclusion

In this thesis, a comparison study was carried out to see the wellbore-reservoir characterization when gas and supercritical CO_2 is injected into an aquifer initially fully saturated with brine – 95% water and 5% NaCl. The results showed that supercritical CO_2 injection has tremendous advantages over gas CO_2 injection.

First, as stated by Roussanaly et al., 2021, CO_2 is usually transported via pipeline in its supercritical state, meaning that, from the economical point of view, no or little efforts should be done if injected in the same state, while for converting it from supercritical to gas, CO_2 must be subjected to higher pressure and temperature changes to achieve the desired injection conditions.

Second, in none of the cases studied in this thesis, hydrates are formed in the near-wellbore area. The injection and initial hydrostatic conditions used in this work did not fall in the region of CO_2 hydrates, as shown in Figure 2.4.4, Figure 3.1.1, respectively.

Third, as seen from Figure 4.2.4, the cooling effect in the near-wellbore area due to JT effect is higher for the gas CO_2 case than for the supercritical CO_2 one. In general, a higher cooling effect can mean that hydrates are more likely to form in the near wellbore area, leading to a reduction of CO_2 injectivity because it increases the flow resistance and local blockage.

Fourth, as seen from Figure 4.2.7, when NaCl is present in a CO_2-H_2O system, salt will precipitate in the near-wellbore area. For the supercritical CO_2 case, the solid saturation is less than for the CO_2 gas injection case, meaning that there is a higher porosity reduction of the porous media when injecting gas CO_2 into a saline aquifer.

Finally, T2Well/ECO2N coupled wellbore-reservoir simulator turned out to be an accurate software to model CO_2 injection in the integrated wellbore-reservoir system, as stated by Burachok et al., 2022. The simulator captures successfully the transient effects happening in both wellbore and reservoir domains. Moreover, the Joule-Thomson effect, heat exchange with the surrounding area, water evaporation, CO_2 dissolution in the aqueous phase were also successfully modelled.

However, the simulator is not out of limitations, such as CO_2 phase transition between liquid and gas or vice-versa. Also, in real operations, prior to CO_2 injection, cushion gas is usually injected to prevent corrosion, which T2Well/ECO2N is not capable of simulating, since it only handles brine-CO_2 system. Moreover, the temperature initial conditions along the wellbore inputted in this work are unrealistic, but necessary to avoid crossing the CO_2 saturation line (phase transition from CO_2 gas to liquid).

Thus, further research is required on this since these processes are crucial during CO_2 long-term geological sequestration. Further work can be done in sensitivity analysis on the key parameters, such as injection pressure and temperature conditions, thermal conductivity of the rock, CO_2 injection mass rate to analyze the multiphase flow behavior. Also, the semi-analytical heat transfer approach between the wellbore and its surrounding can be deactivated to see its impact on the thermal effects.

References

Alkan, H. et al. (2021) 'Engineering design of CO2 storage in saline aquifers and in depleted hydrocarbon reservoirs: similarities and differences', EarthDoc, 39(6). doi:10.3997/1365-2397.fb2021047.

André, L., Azaroual, M. and Menjoz, A. (2009) 'Numerical simulations of the thermal impact of Supercritical CO2 Injection on chemical reactivity in a carbonate Saline Reservoir', Transport in Porous Media, 82(1), pp. 247–274. doi:10.1007/s11242-009-9474-2.

Aziz, K. (1993). 'Reservoir Simulation Grids: Opportunities and Problems'. OnePetro, [online] 45(7). Available at: <https://onepetro.org/JPT/article-abstract/45/07/658/69918/Reservoir-Simulation-Grids-Opportunities-and?redirectedFrom=fulltext> (Accessed: 26 June 2022).

Burachok, O, Kowollik, P., Flores Rivero, F., Barreto Bermudez, Y., Pauyac Estrada, J.K.. (2022) 'Functional comparison of wellbore-reservoir coupling solutions for CO2 Storage Simulations', 83rd EAGE Annual Conference & Exhibition, 2022, pp. 1–5. doi:10.3997/2214-4609.202210475.

Busch, A. et al. (2010) 'The significance of caprock sealing integrity for CO2 Storage', All Days [Preprint]. doi:10.2118/139588-ms.

Creusen, M. (1970) 'Near wellbore effects induced by CO2 injection and the influence on injectivity in depleted Gas Reservoirs'. TU Delft Repositories. Available at: https://repository.tudelft.nl/islandora/object/uuid%3Aa1ee8f04-4b75-45aa-b808-451ab383603d (Accessed: 20 May 2023).

Cui, G. et al. (2023) 'A review of salt precipitation during CO2 injection into saline aquifers and its potential impact on carbon sequestration projects in China', Fuel, 334, p. 126615. doi:10.1016/j.fuel.2022.126615.

Da Silva, D. and Jansen, J. (2015) 'A review of Coupled Dynamic Well-Reservoir Simulation'. ScienceDirect, [online] 48(6). Available at: <https://www.sciencedirect.com/science/article/pii/S2405896315009040> (Accessed: 26 June 2022).

Fanchi, J. (2010) 'Integrated Reservoir Asset Management'. ScienceDirect, pp.125-144.

Gauteplass, J., Almenningen S., Barth T., Ersland G. (2020) 'Hydrate plugging and flow remediation during CO2 Injection in sediments'. [online] Available at: https://doi.org/10.3390/en13174511 (Accessed: 26 June 2022).

Global CCS Institute. (2015) 'Capturing CO2'. [online] Available at: https://www.globalccsinstitute.com/archive/hub/publications/191018/fact-sheet-capturing-co2.pdf (Accessed: 21 April 2022).

Global CCS Institute. (no date) 'Understanding CCS'. [online] Available at: https://www.globalccsinstitute.com/about/what-is-ccs/ (Accessed: 21 April, 2022).

Gor, G.Yu. and Prévost, J.H. (2013) 'Effect of CO2 injection temperature on caprock stability', Energy Procedia, 37, pp. 3727–3732. doi:10.1016/j.egypro.2013.06.267.

Hoteit, H., Fahs, M. and Soltanian, M.R. (2019) 'Assessment of CO2 injectivity during sequestration in depleted Gas Reservoirs', Geosciences, 9(5), p. 199. doi:10.3390/geosciences9050199.

Hu, B. and Chupin, G. (2007) Integrated 'Wellbore-Reservoir Dynamic Simulation'. ResearchGate, [online] Available at: <https://www.researchgate.net/publication/254527072_Integrated_Wellbore-Reservoir_Dynamic_Simulation> (Accessed: 26 June 2022).

Jiang, P. et al. (2014) 'Thermal modeling of CO2 in the injection well and reservoir at the Ordos CCS Demonstration Project, China', International Journal of Greenhouse Gas Control, 23, pp. 135–146. doi:10.1016/j.ijggc.2014.01.011.

Kivi, I.R., Vilarrasa, V. and Makhnenko, R. (2021) Effect of Caprock Relative Permeability on Co2 Flow through it. Available at: https://sintef.brage.unit.no/sintef-xmlui/handle/11250/2785918 (Accessed: 16 September 2023).

Lake, L. (2006). 'Petroleum Engineering Handbook Volume V'. vdoc.pub, pp.1407-1486.

Lawrence Berkeley National Laboratory (1999). 'TOUGH2 User's Guide, Version 2'. [online] Available at: <https://tough.lbl.gov/assets/docs/TOUGH2_V2_Users_Guide.pdf> (Accessed: 26 June 2022).

Lawrence Berkeley National Laboratory (2005). 'ECO2N: A TOUGH2 Fluid Property Module for Mixtures of Water, NaCl, and CO2'. [online] Lawrence Berkeley National Laboratory. Available at: <https://tough.lbl.gov/assets/docs/TOUGH2_ECO2N_Users_Guide.pdf> (Accessed: 26 June 2022).

Lu, M. and Connell, L.D. (2014) 'The transient behaviour of CO 2 flow with phase transition in injection wells during geological storage – application to a case study', Journal of Petroleum Science and Engineering, 124, pp. 7–18. doi:10.1016/j.petrol.2014.09.024.

Magalhães Pires, J. (2019). 'Carbon Capture and Storage'. ResearchGate, [online] Available at: <https://www.researchgate.net/publication/335224308_Carbon_Capture_and_Storage> (Accessed: 12 July 2022).

Mukhopadhyay, S., Yang, S.-Y. and Yeh, H.-D. (2011) 'Pressure buildup during supercritical carbon dioxide injection from a partially penetrating borehole into gas reservoirs', Transport in Porous Media, 91(3), pp. 889–911. doi:10.1007/s11242-011-9879-6.

National Energy Technology Laboratory (no date). 'Carbon Storage Faqs'. [online] Available at: https://netl.doe.gov/carbon-management/carbon-storage/faqs/carbon-storage-faqs (Accessed: 20 July 2022).

NewClimate Institute & Climate Analytics (2020). 'Paris Agreement turning point'. [online] Climate Action Tracker. Available at: <https://climateactiontracker.org/documents/829/CAT_2020-12-01_Briefing_GlobalUpdate_Paris5Years_Dec2020.pdf> (Accessed: 12 July 2022).

NIST Chemistry Webbook. n.d. 'Saturation Properties for Carbon dioxide — Temperature Increments'. [online] Available at: <https://webbook.nist.gov/cgi/fluid.cgi?TLow=-56.558&THigh=30.9782&TInc=5&Applet=on&Digits=5&ID=C124389&Action=Load&Type=SatP&TUnit=C&PUnit=bar&DUnit=kg%2Fm3&HUnit=kJ%2Fmol&WUnit=m%2Fs&VisUnit=Pa*s&STUnit=N%2Fm&RefState=DEF> (Accessed: 13 May 2022).

Pan, L., Oldenburg, C., Wu, Y. and Pruess, K. (2011) 'T2Well/ECO2N Version 1.0.: Multiphase and Non-Isothermal Model for Coupled Wellbore-Reservoir Flow of Carbon Dioxide and Variable Salinity Water. ResearchGate'. [online] Available at: <https://www.researchgate.net/publication/255222772_T2WellECO2N_Version_10_Multiphase_and_Non-Isothermal_Model_for_Coupled_Wellbore-Reservoir_Flow_of_Carbon_Dioxide_and_Variable_Salinity_Water> (Accessed: 26 June 2022).

Paterson, L., Ennis-King, J. and Sharma, S. (2010) 'Observations of thermal and pressure transients in carbon dioxide wells', All Days. doi:10.2118/134881-ms.

Petroleum Experts (2013). 'User Manual PROSPER'. SCRIBD [online] Available at: <https://www.scribd.com/document/220173287/PROSPER-complete-pdf> (Accessed: 19 July 2022).

Pruess, K., 2011. ECO2M: 'A TOUGH2 Fluid Property Module for Mixtures of Water, NaCl, and CO2, Including Super- and Sub-Critical Conditions, and Phase Change Between Liquid and Gaseous CO2'. ResearchGate, [online] Available at: <https://www.researchgate.net/publication/241970891_ECO2M_A_TOUGH2_Fluid_Property_Module_for_Mixtures_of_Water_NaCl_and_CO2_Including_Super_and_SubCritical_Conditions_and_Phase_Change_Between_Liquid_and_Gaseous_CO2> (Accessed: 26 June 2022).

Pruess, K. (2009) 'Formation dry-out from CO2injection into saline aquifers: 2. analytical model for salt precipitation', Water Resources Research, 45(3). doi:10.1029/2008wr007102.

Raza, A., Gholami, R., Reza, R., Rasouli, V., Rabiei, M. (2018). 'Significant Aspects of Carbon Capture and Storage – A Review'. ResearchGate, [online] Available at: <https://www.researchgate.net/publication/329714495_Significant_Aspects_of_Carbon_Capture_and_Storage_-_A_Review> (Accessed 12 July 2022).

Revelation, J.S. (2017). 'Transient flow modelling of start-up CO2 injection into highly-depleted oil/gas fields'. University College London. Available at: https://discovery.ucl.ac.uk/id/eprint/10080137/ (Accessed: 10 June 2023).

Ritchie, H., Roser, M. and Rosado, P, (2020). 'CO2 emissions', Our World in Data. Available at: https://ourworldindata.org/co2-emissions (Accessed: 19 May 2023).

Roussanaly, S. et al. (2021) 'At what pressure shall CO2 be transported by ship? an in-depth cost comparison of 7 and 15 barg shipping', Energies, 14(18), p. 5635. doi:10.3390/en14185635.

Ruan, B. et al. (2013) 'Flow and thermal modeling of CO2 in injection well during geological sequestration', International Journal of Greenhouse Gas Control, 19, pp. 271–280. doi:10.1016/j.ijggc.2013.09.006.

Santim, C.G.S., Fulchignoni, L.P., Rosa, E.S., Gaspari, E.F. (2020) 'Transient multiphase flow modeling and validation in a real production system with high CO2 content using the drift-flux model', Journal of Petroleum Science and Engineering, 188, p. 106903. doi:10.1016/j.petrol.2020.106903.

Seo, Y. et al. (2016) 'Comparison of CO 2 liquefaction pressures for ship-based carbon capture and storage (CCS) chain', International Journal of Greenhouse Gas Control, 52, pp. 1–12. doi:10.1016/j.ijggc.2016.06.011.

Singh, U., (2013). 'Carbon capture and storage: An effective way to mitigate global warming'. ResearchGate, [online] Available at: <https://www.researchgate.net/publication/270159236_Carbon_capture_and_storage_An_effective_way_to_mitigate_global_warming> (Accessed: 12 July 2022).

Sokama-Neuyam, Y.A. et al. (2022) 'The effect of temperature on CO2 injectivity in Sandstone Reservoirs', Scientific African, 15. doi:10.1016/j.sciaf.2021.e01066.

Vasini, E.M., Battistelli A., Berry P., Bonduà S., Bortolotti V., Cormio C., Pan L., (2015). 'Interpretation of production tests in geothermal wells with T2WELL-EWASG,' Geothermics [Online]. Available at: <https://doi.org/10.1016/j.geothermics.2017.06.005> (Accessed 12 July 2022).

Vilarrasa, V. et al. (2013) 'Liquid CO2 Injection for geological storage in deep saline aquifers', International Journal of Greenhouse Gas Control, 14, pp. 84–96. doi:10.1016/j.ijggc.2013.01.015.

Wan, N.-H. et al. (2021) Modeling transient flow in CO2 Injection Wells by considering the phase change, MDPI. Available at: https://www.mdpi.com/2227-9717/9/12/2164 (Accessed: 19 May 2023).

Witkowski, A., Majkut, M. and Rulik, S., 2014. Analysis of pipeline transportation systems for carbon dioxide sequestration. ResearchGate, [online] Available at: <https://www.researchgate.net/publication/267328310_Analysis_of_pipeline_transp ortation_systems_for_carbon_dioxide_sequestration> (Accessed: 26 June 2022).

Zamani N. et al. Evaluation of wellbore-reservoir response in coupled CO2 storage simulation (pre-print).

Zamani N., C. M. Oldenburg, Solbakken J., Aaarra M. G., Kowollik P, Alkan H., Amro M., Nassan T., Pauyac Estrada J. K., Burachok O. (2023). 'CO2 Flow Modeling in a Coupled Wellbore and Aquifer System: Details of Pressure, Temperature, and Dry-Out' [preprinted].

Zapata, Y., Kristensen M. R., Huerta N., Brown C., Kabir C. S., Reza Z. (2022) 'Well-based monitoring of CO2 geological sequestration operations in saline aquifers: Critical insights into key questions', Carbon Capture Science & Technology, 5, p. 100079. doi:10.1016/j.ccst.2022.100079.

Zhang, Y. et al. (2011) 'A Time-convolution approach for modeling heat exchange between a wellbore and surrounding formation', Geothermics, 40(4), pp. 261–266. doi:10.1016/j.geothermics.2011.08.003.

Ziabakhsh-Ganji, Z. and Kooi, H. (2013) 'Sensitivity of joule–thomson cooling to impure CO2 injection in depleted Gas Reservoirs,' ELSEVIER [online]. Available at: https://doi.org/10.1016/j.apenergy.2013.07.059 [Accessed 8 March 2023].

List of Figures

List of Tables

Nomenclature

t	Time	[s]
p	Pressure	[Pa]

Abbreviations

CCS	Carbon Capture and Storage
GPAS	General Purpose Adaptive Simulator
CMG	Computer Modelling Group
JT	Joule-Thomson
PROSPER	Production System Performance
NIST	National Institute of Standards and Technology
BC	Boundary Conditions